

Synthesis, Structural-Bonding Magnetic Study, and ^1H NMR Analysis of the Temperature-Dependent Singlet–Triplet Solution Equilibrium of the 46-Electron Tricobalt Tris(pentamethylcyclopentadienyl) Dicarbonyl, $\text{Co}_3(\eta^5\text{-C}_5\text{Me}_5)_3(\mu_3\text{-CO})_2$: An Isolobal Analogue of the Elusive Antiaromatic Cyclopropenyl Monoanion

William L. Olson,^{1a,b} Angelica M. Stacy,^{1c} and Lawrence F. Dahl*^{1b}

Contribution from the Department of Chemistry, University of Wisconsin—Madison, Madison, Wisconsin 53706, and the Department of Chemistry, University of California, Berkeley, California 94720. Received September 12, 1985

Abstract: In an extension of our structural-bonding analyses of the classical 49-electron Fischer–Palm $\text{Ni}_3(\eta^5\text{-C}_5\text{H}_5)_3(\mu_3\text{-CO})_2$ and related derivatives, we have isolated the corresponding 46-electron $\text{Co}_3(\eta^5\text{-C}_5\text{Me}_5)_3(\mu_3\text{-CO})_2$ (**1**). This highly air-sensitive molecular compound was characterized from mass spectral, IR, electrochemical, temperature-variable solid-state magnetic susceptibility, temperature-variable ^1H NMR, and X-ray diffraction measurements. Obtained as a minor product (1–2% yield) of the photolytic decomposition of $\text{Co}(\eta^5\text{-C}_5\text{Me}_5)(\text{CO})_2$, this electron-deficient cluster is the first example of a multiple-bonded trinuclear metal system containing only first-row transition-metal atoms. A magnetic susceptibility study carried out with a SQUID magnetometer at magnetic fields from 1 to 40 kG and over a temperature range of 4 to 280 K showed that in the solid state **1** does not have two unpaired electrons as predicted by theory (under assumed threefold symmetry). Proton NMR spectra of **1** in toluene- d_8 solution exhibited a dramatic temperature dependence with the single observed methyl proton resonance shifting from a paramagnetic-induced value of δ 3.44 at 22 °C to a diamagnetic-limiting value of δ 1.78 at –95 °C. The temperature-dependent isotropic-shift data for the proton resonance were analyzed on the basis of a singlet–triplet equilibrium in solution for **1** and were found to give an excellent fit to a generalized form of the contact-shift equation over the entire temperature range of –95 to +97 °C. Both **1** and the electronically equivalent $\text{Rh}_3(\eta^5\text{-C}_5\text{Me}_5)_3(\mu_3\text{-CO})_2$ (**2**), which was recently synthesized by Stone and co-workers and independently in our laboratories and which was characterized by Howard from a low-temperature X-ray diffraction investigation, are representative of only a few known electronically unsaturated triangular metal clusters. The structural-bonding interrelationships of **1**, **2**, and the isolobal (but non-isolatable) cyclopropenyl monoanion, which is the simplest known 4π electron, antiaromatic triplet-state species under D_{3h} symmetry, were examined. Although all three of these triangular ring systems possess the same triplet ground state (viz., $^3A'_2$) under assumed D_{3h} symmetry with two unpaired electrons, each appears to undergo a different geometrical distortion in order to remove the degeneracy of the two half-filled HOMOs and thereby give a singlet ground state. For the $[\text{C}_3\text{H}_3]^-$ monoanion, reported nonempirical MO calculations point to a nonplanar C_s – m geometry with two carbon atoms forming an ethylenic π bond and with a third highly pyramidalized carbon atom bearing a localized electron pair. In the low-temperature crystal structure of **2**, the $\text{Rh}_3(\text{CO})_2$ core of crystallographic C_1 –1 site symmetry closely conforms to a C_{2v} – $2mm$ geometry with Rh–Rh and Rh–CO bond-length differences of 0.08 and 0.36 Å, respectively; this pronounced C_{2v} deformation from D_{3h} symmetry is in accordance with its diamagnetic character in solution. In sharp contrast, the solid-state structure of **1**, which possesses crystallographic C_{3h} – $3/m$ site symmetry, provides no evidence that the atomic thermal ellipsoids are a threefold composite of a substantially distorted $\text{Co}_3(\text{CO})_2$ core of either C_{2v} or C_3 symmetry. Hence, it is hypothesized that the relatively low magnetic moment (e.g., 0.97 and 0.73 μ_B at 280 and 200 K, respectively) of **1** in the solid state arises primarily from instantaneous deformations (of non-threefold molecular symmetry) of the C_5Me_5 rings from regular pentagonal symmetry such that the resulting nonequivalent Co atoms split the degeneracy of the two half-filled HOMOs; a crystallographically indicated distortion is observed for the mirror-bisected C_5Me_5 rings which are assumed to be disordered in the threefold-averaged configuration. Also reported is the 48-electron $\text{Co}_3(\eta^5\text{-C}_5\text{Me}_5)_3(\mu_3\text{-CO})(\mu_3\text{-O})$ (**3**) which was isolated as a side product (~1% yield) in the preparation of **1** and which was characterized from mass spectral, ^1H NMR, IR, and electrochemical measurements. $\text{Co}_3(\eta^5\text{-C}_5\text{Me}_5)_3(\mu_3\text{-CO})_2$ (**1**): formula weight = 638.5; hexagonal; $P6_3/m$; $a = b = 10.636$ (3) Å, $c = 15.294$ (7) Å, $V = 1498$ (1) Å³ at $T = 295$ K; $D(\text{calcd}) = 1.39$ g/cm³ for $Z = 2$. Least-squares refinement converged at $R_1(F) = 3.78\%$, $R_2(F) = 5.73\%$ for 621 independent diffractometry data ($I > 2.5\sigma(I)$) with a data-to-parameter ratio of 10.5/1.

Metal-fragment additions to metal–metal multiple-bonded dimers are a rapidly expanding and significant part of metal cluster chemistry.^{2–10} Such reactions, which provide rational synthetic

routes to a wide variety of mixed metal cluster systems, are especially interesting not only with respect to possible heterometallic catalyst design but also in extending our knowledge of comparative metal–metal multiple-bond reactivities. The comprehensive work by Stone and co-workers,^{3–10} including their use of organometallic reagents with labile ligands to generate electronically unsaturated metal-fragment species for thermal insertion reactions, has had a major impact in this area.

Our entry into this field involved the “net” addition of photochemically generated 16-electron $\text{M}(\text{CO})_{x-1}$ fragments across the

(1) (a) Based in part on the Ph.D. Thesis of W. L. Olson at the University of Wisconsin—Madison, Dec 1984. (b) University of Wisconsin—Madison. (c) University of California—Berkeley.

(2) Cirjak, L. M.; Huang, J.-S.; Zhu, Z.-H.; Dahl, L. F. *J. Am. Chem. Soc.* **1980**, *102*, 6623–6626.

(3) Green, M.; Mills, R. M.; Pain, G. N.; Stone, F. G. A.; Woodward, P. *J. Chem. Soc., Dalton Trans.* **1982**, 1309–1319.

(4) Boag, N. M.; Green, M.; Mills, R. M.; Pain, G. N.; Stone, F. G. A.; Woodward, P. *J. Chem. Soc., Chem. Commun.* **1980**, 1171–1173.

(5) Stone, F. G. A. *Angew. Chem., Int. Ed. Engl.* **1984**, *23*, 89–99.

(6) Farrugia, L. J.; Howard, J. A. K.; Mitrprachachon, P.; Stone, F. G. A.; Woodward, P. *J. Chem. Soc., Dalton Trans.* **1981**, 155–161.

(7) Farrugia, L. J.; Howard, J. A. K.; Mitrprachachon, P.; Stone, F. G. A.; Woodward, P. *J. Chem. Soc., Dalton Trans.* **1981**, 171–179.

(8) Brun, P.; Dawkins, G. M.; Green, M.; Miles, A. D.; Orpen, A. G.; Stone, F. G. A. *J. Chem. Soc., Chem. Commun.* **1982**, 926–927.

(9) Barr, R. D.; Green, M.; Howard, J. A. K.; Marder, T. B.; Stone, F. G. A. *J. Chem. Soc., Chem. Commun.* **1983**, 759–760.

(10) Green, M.; Hankey, D. R.; Howard, J. A. K.; Louca, P.; Stone, F. G. A. *J. Chem. Soc., Chem. Commun.* **1983**, 757–758.

Co–Co double bond of the 32-electron $\text{Co}_2(\eta^5\text{-C}_5\text{Me}_5)_2(\mu_2\text{-CO})_2$,¹¹ a series of 48-electron triangular metal clusters corresponding to the general formula $\text{MCo}_2(\eta^5\text{-C}_5\text{Me}_5)_2(\mu_2\text{-CO})_x(\mu_3\text{-CO})$ (where for $x = 2$, $\text{M} = \text{Fe}(\text{CO})_3$ or $\text{Co}(\eta^5\text{-C}_5\text{H}_4\text{Me})$ and for $x = 3$, $\text{M} = \text{Cr}(\eta^5\text{-C}_6\text{H}_5\text{Me})$, $\text{Mn}(\eta^5\text{-C}_5\text{H}_4\text{Me})$, or $\text{Fe}(\eta^4\text{-C}_4\text{H}_4)$) was obtained from these reactions and characterized by spectroscopic and X-ray diffraction measurements. An important advantage of this metal-fragment insertion route for the synthesis of mixed metal clusters was that the products were isolated in relatively high yields. These insertion reactions may be viewed from the isolobal model^{5,12} as corresponding to the cycloaddition of a methylene fragment to ethylene to give cyclopropane.

We have made further efforts to expand the chemistry of $\text{Co}_2(\eta^5\text{-C}_5\text{Me}_5)_2(\mu_2\text{-CO})_2$ by reacting it with a number of other electronically deficient metal fragments. As part of these investigations an attempt was made to prepare an iron–dicobalt cluster by the cycloaddition of the methylene-like 16-electron $\text{Fe}(\eta^5\text{-C}_5\text{H}_5)(\text{CO})\text{Me}$ fragment,¹³ photogenerated from $\text{Fe}(\eta^5\text{-C}_5\text{H}_5)(\text{CO})_2\text{Me}$, to the ethylene-like $\text{Co}_2(\eta^5\text{-C}_5\text{Me}_5)_2(\mu_2\text{-CO})_2$. Although not successful in isolating the desired product, we were surprised by the initial isolation from this reaction of $\text{Co}_3(\eta^5\text{-C}_5\text{Me}_5)_3(\mu_3\text{-CO})_2$ (**1**), a tricobalt pentamethylcyclopentadienyl analogue of the Fischer–Palm 49-electron $\text{Ni}_3(\eta^5\text{-C}_5\text{H}_5)_3(\mu_3\text{-CO})_2$. This 46-electron trimetal cluster is the first example of a metal–metal multiple-bonded triangular metal cluster containing only first-row transition-metal atoms.¹⁴ Its formation may be conceptually viewed as arising from the cycloaddition of the 14-electron $\text{Co}(\eta^5\text{-C}_5\text{Me}_5)$ fragment to the 32-electron $\text{Co}_2(\eta^5\text{-C}_5\text{Me}_5)_2(\mu_2\text{-CO})_2$. We were particularly interested in the structural-bonding features of this highly unusual tricobalt cluster because it is isolobal with the non-isolated cyclopropenyl monoanion, the simplest known 4π -electron, antiaromatic species (under D_{3h} symmetry).^{15,16} This $[\text{C}_3\text{H}_3]^-$ monoanion has been the subject of extensive theoretical analyses¹⁷ due to its conceptual existence as a planar D_{3h} diradical with a triplet ground state; deformations to less symmetrical equilibrium geometries (planar and nonplanar) with concomitant singlet ground states have been proposed from ab initio MO calculations.¹⁷

At approximately the same time as our discovery¹⁴ of **1**, we also isolated its trirhodium analogue, $\text{Rh}_3(\eta^5\text{-C}_5\text{Me}_5)_3(\mu_3\text{-CO})_2$ (**2**), from the photolytic reaction of $\text{Co}_2(\eta^5\text{-C}_5\text{Me}_5)_2(\mu_2\text{-CO})_2$ with $\text{Rh}_2(\eta^5\text{-C}_5\text{Me}_5)_2(\mu_2\text{-CO})_2$,¹⁸ from which we hoped to obtain the 60-electron $\text{Co}_2\text{Rh}_2(\eta^5\text{-C}_5\text{Me}_5)_4(\mu_3\text{-CO})_2$. A room-temperature X-ray diffraction analysis¹⁴ of $\text{Rh}_3(\eta^5\text{-C}_5\text{Me}_5)_3(\mu_3\text{-CO})_2$ revealed a crystal-disordered averaged structure whose refined parameters proved to be of little value in unraveling the actual configuration of the $\text{Rh}_3(\text{CO})_2$ core. Independently, Stone and co-workers¹⁹ reported the synthesis of the same trirhodium cluster and corre-

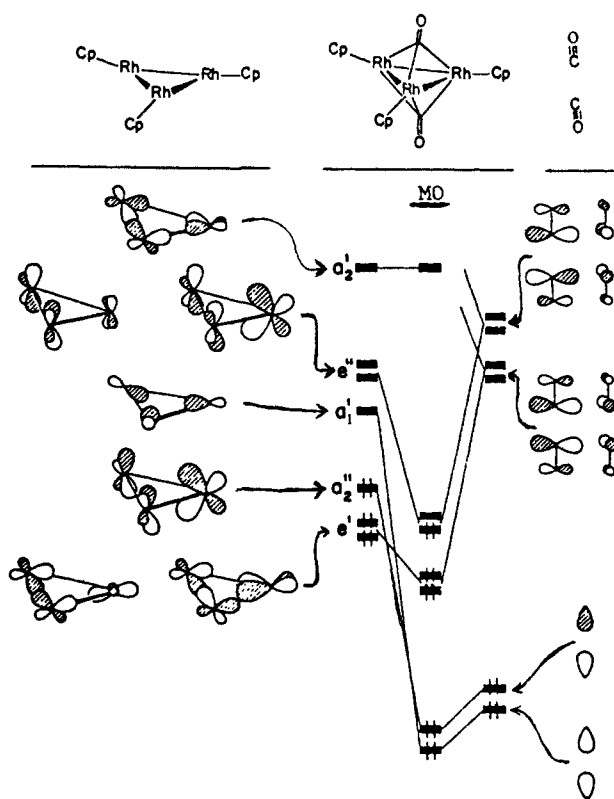


Figure 1. Molecular orbital correlation diagram presented by Pinhas, Albright, Hofmann, and Hoffmann²⁴ in 1980 for a hypothetical 46-electron $\text{Rh}_3(\eta^5\text{-C}_5\text{H}_5)_3(\mu_3\text{-CO})_2$ molecule, which under D_{3h} symmetry was proposed to be an open-shell complex with two unpaired electrons. This theoretical analysis preceded the syntheses and characterizations of the 46-electron $\text{M}_3(\eta^5\text{-C}_5\text{Me}_5)_3(\mu_3\text{-CO})_2$ ($\text{M}_3 = \text{Rh}_3, \text{CoRh}_2, \text{Co}_3$) clusters.

sponding cobalt–dirhodium analogue of general formula $\text{Co}_x\text{Rh}_{3-x}(\eta^5\text{-C}_5\text{Me}_5)_3(\mu_3\text{-CO})_2$ (where $x = 0, 1$) from the thermal reaction of $\text{M}(\eta^5\text{-C}_5\text{Me}_5)(\text{C}_2\text{H}_4)_2$ (where $\text{M} = \text{Co}, \text{Rh}$) with the $\text{Rh}_2(\eta^5\text{-C}_5\text{Me}_5)_2(\mu_2\text{-CO})_2$ dimer. A low-temperature X-ray diffraction study by Howard^{20a} of $\text{Rh}_3(\eta^5\text{-C}_5\text{Me}_5)_3(\mu_3\text{-CO})_2$ (**2**) disclosed a crystal-ordered structure. Details of this structural determination together with syntheses of the tricobalt,²¹ rhodium–dicobalt, and iridium–dicobalt analogues were recently reported by Stone and co-workers.^{20b,22} They also found that the trirhodium cluster and the related cobalt– and iridium–dirhodium complexes react with dihydrogen to give $\text{MRh}_2(\eta^5\text{-C}_5\text{Me}_5)_3(\mu_2\text{-H})_2(\mu_2\text{-CO})(\mu_3\text{-CO})$ complexes ($\text{M} = \text{Co}, \text{Rh}, \text{Ir}$), of which the molecular structure of the dihydridotrirhodium cluster was

(11) Cirjak, L. M.; Ginsburg, R. E.; Dahl, L. F. *Inorg. Chem.* **1982**, *21*, 940–957.

(12) (a) Elian, M.; Chen, M. M. L.; Mingos, D. M. P.; Hoffmann, R. *Inorg. Chem.* **1976**, *15*, 1148–1155. (b) Hoffmann, R. *Science (Washington, D.C.)* **1981**, *211*, 995–1002. (c) Hoffmann, R. *Angew. Chem., Int. Ed. Engl.* **1982**, *21*, 711–724. (d) Albright, T. A. *Tetrahedron* **1982**, *38*, 1339–1388.

(13) Kazlauskas, R. J.; Wrighton, M. S. *Organometallics* **1982**, *1*, 602–611.

(14) Olson, W. L.; Schugart, K. A.; Fenske, R. F.; Dahl, L. F. *Abstracts of Papers*, 187th National Meeting of the American Chemical Society, St. Louis, Missouri; American Chemical Society: Washington, DC, 1984; INOR 279.

(15) The fleeting existence of the $[\text{C}_3\text{H}_3]^-$ monoanion has been indicated only from a two-electron electrochemical reversible reduction of the cyclopropenyl monoanion.^{16a} No derivatives of this monoanion have been isolated; a $\text{p}K_a$ of 61 has been estimated^{16b} for its conjugate acid, cyclopropene.

(16) (a) Wasielewski, M. R.; Breslow, R. *J. Am. Chem. Soc.* **1976**, *98*, 4222–4229. (b) Breslow, R.; Balasubramanian, K. *J. Am. Chem. Soc.* **1969**, *91*, 5182–5183.

(17) (a) Breslow, R. *Angew. Chem., Int. Ed. Engl.* **1968**, *7*, 565–570. (b) Clark, D. T. *J. Chem. Soc., Chem. Commun.* **1969**, 637–638. (c) Breslow, R. *Acc. Chem. Res.* **1973**, *6*, 393–398. (d) Davidson, E. R.; Borden, W. T. *J. Chem. Phys.* **1977**, *67*, 2191–2200. (e) Borden, W. T.; Davidson, E. R.; Feller, D. *J. Am. Chem. Soc.* **1980**, *102*, 5302–5311. (f) Borden, W. T.; Davidson, E. R. *Acc. Chem. Res.* **1981**, *14*, 69–76.

(18) Nutton, A.; Maitlis, P. M. *J. Organomet. Chem.* **1979**, *166*, C21–C22. (19) Green, M.; Hankey, D. R.; Howard, J. A. K.; Louca, P.; Stone, F. G. A. *J. Chem. Soc., Chem. Commun.* **1983**, 757–758.

(20) (a) Howard, J. A. K., private communication to L. F. Dahl (Nov. 1983). (b) Bray, A. C.; Green, M.; Hankey, D. R.; Howard, J. A. K.; Johnson, O.; Stone, F. G. A. *J. Organomet. Chem.* **1985**, *281*, C12–C16.

(21) Their preparation of $\text{Co}_3(\eta^5\text{-C}_5\text{Me}_5)_3(\mu_3\text{-CO})_2$ (**1**) resulted from the reaction of a mixture of equimolar amounts of $\text{Co}_2(\eta^5\text{-C}_5\text{Me}_5)_2(\mu_2\text{-CO})_2$ and $\text{Co}(\eta^5\text{-C}_5\text{Me}_5)(\text{C}_2\text{H}_4)_2$ in refluxing toluene.^{20b} They also reported for **1** that an infrared spectrum (in THF) exhibited a $\nu_{\text{max}}(\text{CO}) = 1675 \text{ cm}^{-1}$ and that a ^1H NMR spectrum (in C_6D_6) displayed a resonance at δ 3.38 (s, 45 H, C_5Me_5).

(22) (a) Herrmann et al.^{22b} recently reported the synthesis of the 46-electron $(\eta^5\text{-C}_5\text{Me}_5)\text{IrCo}_2(\eta^5\text{-C}_5\text{H}_5)_2(\mu_3\text{-CO})_2$ in high yield by the “net” cycloaddition of the 14-electron $\text{Co}(\eta^5\text{-C}_5\text{H}_5)$ fragment, generated from $\text{Co}(\eta^5\text{-C}_5\text{H}_5)(\text{C}_2\text{H}_4)_2$, across the Ir–Co double bond of the 32-electron $(\eta^5\text{-C}_5\text{Me}_5)\text{IrCo}_2(\eta^5\text{-C}_5\text{H}_5)_2(\mu_2\text{-CO})_2$. A crystallographic investigation of this highly reactive IrCo₂ cluster revealed a highly distorted solid-state geometry with two short Co–Co and Ir–Co distances of 2.359 (1) and 2.473 (1) Å and one longer Ir–Co distance of 2.527 (1) Å. In startling contrast to the 46-electron $\text{Co}_3(\eta^5\text{-C}_5\text{Me}_5)_3(\mu_3\text{-CO})_2$ (**1**) and $\text{Rh}_3(\eta^5\text{-C}_5\text{Me}_5)_3(\mu_3\text{-CO})_2$ (**2**) clusters, the 46-electron IrCo₂ cluster contains two unpaired electrons in the crystalline state, as evidenced by a magnetic moment of 4.06 μ_B obtained at room temperature by the Faraday method. Furthermore, temperature-dependent ^1H NMR spectra conclusively show that the triplet ground state (which from symmetry considerations must be accidental) persists in solution (benzene- d_6 or toluene- d_8) over the temperature range of –93 to +100 °C. (b) Herrmann, W. A.; Barnes, C. E.; Zahn, T.; Ziegler, M. L. *Organometallics*, **1985**, *4*, 172–180.

established by X-ray diffraction.^{20b}

Prior to these syntheses, theoretical predictions were made first by Schilling and Hoffmann²³ and shortly thereafter by Pinhas, Albright, Hofmann, and Hoffmann²⁴ concerning the electronic structures of the unknown 46-electron $M_3(\eta^5-C_5H_5)_3(\mu_3-CO)_2$ clusters ($M = Co$,²³ Rh ²⁴). Molecular orbital calculations via the extended-Hückel method on the hypothetical cyclopentadienyl analogue, $Rh_3(\eta^5-C_5H_5)_3(\mu_3-CO)_2$,²⁴ suggested that this molecule should possess two unpaired electrons in two doubly degenerate, half-filled e'' HOMOs under D_{3h} symmetry (Figure 1). It was also pointed out²⁴ that $Rh_3(\eta^5-C_5H_5)_3(\mu_3-CO)_2$ could either remain a symmetrical high-spin species or distort in some fashion (e.g., by deformation of either the C_5H_5 rings and/or the $Rh_3(CO)_2$ core) in order to lift the degeneracy of the e'' HOMOs.

Presented herein are the full details of our synthesis and physicochemical measurements of **1**, including a magnetic susceptibility study in the solid state and an analysis of its observed temperature-dependent equilibrium between singlet and triplet spin states in solution. The structural-bonding interrelationships between **1**, its trirhodium analogue (**2**), and its isolobal organic counterpart, the cyclopropenyl monoanion, are given. The isolation and properties of a biproduct, the 48-electron $Co_3(\eta^5-C_5Me_5)_3(\mu_3-CO)(\mu_3-O)$, are also described. The results of nonparametrized MO calculations on hypothetical cyclopentadienyl derivatives of **1** and **2** with undistorted (D_{3h}) and distorted (C_{2v}) trimetal dicarbonyl geometries will be presented elsewhere; a preliminary account of this theoretical study has been given.¹⁴

Experimental Section

General Techniques and Materials. All reactions and manipulations were carried out under an atmosphere of dry nitrogen via standard Schlenk-ware techniques or within a Vacuum Atmospheres drybox. The following solvents were dried and distilled immediately before use: hexane (CaH_2), toluene (sodium benzophenone ketyl), acetone (B_2O_3), dichloromethane (P_2O_5), tetrahydrofuran (potassium benzophenone ketyl), and acetonitrile (CaH_2). Deuterated solvents, e.g., benzene- d_6 (CaH_2), toluene- d_8 (CaH_2), and acetone- d_6 (molecular sieves), were frozen and then degassed three times and vacuum-distilled before use. $Co(\eta^5-C_5Me_5)(CO)_2$ was prepared via the general method of Rausch and Genetti²⁵ by the reaction of $Co_2(CO)_8$ (Strem) with C_5Me_5H in refluxing CH_2Cl_2 . Pentamethylcyclopentadiene²⁶ and $[Co(\eta^5-C_5Me_5)_2]_2$ ²⁷ were prepared in accordance with literature methods. All other reagents were purchased from major chemical suppliers and used without further purification.

Synthesis. (a) Initial Isolation of $Co_3(\eta^5-C_5Me_5)_3(\mu_3-CO)_2$ (1**).** An attempted cycloaddition of an $Fe(\eta^5-C_5H_5)(CO)Me$ fragment to $Co_2(\eta^5-C_5Me_5)_2(\mu_2-CO)_2$ gave rise to **1** as a low-yield side product. A solution of $Co_2(\eta^5-C_5Me_5)_2(\mu_2-CO)_2$ ¹¹ (0.5 g, 1.1 mmol) and $Fe(\eta^5-C_5H_5)(CO)_2Me$ ¹³ (0.5 g, 2.6 mmol) in toluene (150 mL) was photolyzed in a Pyrex glass apparatus which was continually purged with nitrogen to facilitate the removal of evolved carbon monoxide. Periodic monitoring of the solution by infrared spectroscopy revealed the rapid formation of $Fe_2(\eta^5-C_5H_5)_2(CO)_2(\mu_2-CO)_2$ as a major product. After 1.5 h, the photolysis was discontinued and the solvent removed under vacuum. The residue was extracted with 30 mL of hexane, and a small portion was removed for IR analysis. The resulting spectrum was extremely complicated, but the major peaks were readily assigned to $Co(\eta^5-C_5Me_5)(CO)_2$, $Co_2(\eta^5-C_5Me_5)_2(\mu_2-CO)_2$, and the aforementioned iron dimer. Extraction of the residue with hexane followed by chromatography on alumina yielded several bands. Fractional crystallization of two of these bands yielded small quantities (ca. 2–3% yield) of **1** and $Fe_2Co(\eta^5-C_5H_5)_2(\eta^5-C_5Me_5)(CO)_4$,²⁸ the latter compound was unambiguously identified from a preliminary X-ray crystallographic analysis.

(b) Preparation of $Co(\eta^5-C_5Me_5)(C_2H_4)_2$. In a typical reaction,²⁹ an amalgam of Na (200 mg, 8.6 mmol) in 2 mL of Hg was prepared in a 250-mL round-bottomed flask and then mixed with 40 mL of a 90/10 mixture (v/v) of diethyl ether and tetrahydrofuran. After the system was

rapidly purged with ethylene (Matheson), solid $[Co(\eta^5-C_5Me_5)_2]_2$ (0.3 g, 0.22 mmol) was slowly added with rapid stirring. Reaction of the resulting suspension for 1 h at room temperature yielded a red solution. The solution was decanted, the solvent was rapidly removed under vacuum, and the residue was extracted with 20-mL portions of hexane. The resultant red solution of $Co(\eta^5-C_5Me_5)(C_2H_4)_2$ was placed under an atmosphere of ethylene and cooled with dry ice until needed.

(c) Attempted Photochemical Preparation of **1 from $Co_2(\eta^5-C_5Me_5)_2(\mu_2-CO)_2$ and $Co(\eta^5-C_5Me_5)(C_2H_4)_2$.** The $Co_2(\eta^5-C_5Me_5)_2(\mu_2-CO)_2$ dimer (150 mg, 0.3 mmol) was dissolved in toluene (100 mL) and transferred to a Pyrex photolysis apparatus under nitrogen. During photolysis with a 450-W Hanovia medium pressure mercury lamp, a 20-mL hexane solution of $Co(\eta^5-C_5Me_5)(C_2H_4)_2$ (0.1 g, 0.4 mmol) was added over a 1-h period, after which the irradiation was discontinued and the solvent removed under vacuum. Extraction of the green residue with hexane (20 mL) revealed small amounts of an insoluble precipitate which was believed to arise from the decomposition of $Co(\eta^5-C_5Me_5)(C_2H_4)_2$. Infrared spectral analysis of a small portion of the extract showed no evidence for **1** (i.e., a characteristic absorption peak at 1685 cm^{-1} was absent); an intense band at 1760 cm^{-1} indicated the presence of a large amount of starting dimer.

(d) Attempted Thermal Preparation of **1 from $Co_2(\eta^5-C_5Me_5)_2(\mu_2-CO)_2$ and $Co(\eta^5-C_5Me_5)(C_2H_4)_2$.** To a solution of hexane 0.150 g (0.3 mmol) of $Co_2(\eta^5-C_5Me_5)_2(\mu_2-CO)_2$ in 30 mL of hexane was added 0.1 g (0.4 mmol) of red-orange crystalline $Co(\eta^5-C_5Me_5)(C_2H_4)_2$. The solution was stirred at room temperature, and small portions were periodically removed for infrared spectral analysis. Decomposition of olefin reactant was evident from the formation of an insoluble precipitate during the reaction. A substantial amount of **1** was not observed to form over a 1-h period. Attempts to improve the synthesis by a cooling or heating of the reaction vessel were also unsuccessful.

(e) Preparation of $Co_3(\eta^5-C_5Me_5)_3(\mu_3-CO)_2$ (1**).** A solution of $Co(\eta^5-C_5Me_5)(CO)_2$ (0.5 g, 2 mmol) in hexane (125 mL) was photolyzed in a Pyrex glass apparatus continually purged with a slow flow of nitrogen to facilitate the removal of evolved carbon monoxide. After 24 h, an infrared spectrum of the reaction mixture indicated that all of the cobalt starting material had been consumed. The hexane solution was reduced in volume and carefully loaded onto a chromatographic column containing oxygen-free alumina (activity grade 1, Brockman 80–200 mesh, Fischer Scientific). Slow elution with hexane over a 4-h period led to the formation of a dark green band of $Co_2(\eta^5-C_5Me_5)_2(\mu_2-CO)_2$ followed closely by a dark brown band of **1**. The bands were then rapidly eluted off the column with toluene. Vacuum removal of the solvent from the brown band gave (in each of several runs) ca. 10–20 mg of a black microcrystalline solid identified as **1** (0.8–2.0% yield).

Occasionally, a second dark brown band was observed to remain at the top of the column. This band was easily eluted with a 20/80 mixture of THF/toluene (v/v); a high-resolution mass spectrometric analysis showed it to be $Co_3(\eta^5-C_5Me_5)_3(\mu_3-CO)(\mu_3-O)$ (**3**).

Characterization of $Co_3(\eta^5-C_5Me_5)_3(\mu_3-CO)_2$ (1**).** **(a) Properties and Infrared Data.** This extremely air-sensitive compound readily decomposes when in contact with either air or water. However, solutions of **1** are stable for an indefinite time when solvents are rigorously purified and the storage vessel is hermetically sealed. The dark colored compound crystallizes readily from hexane and is very soluble in common organic solvents such as aliphatic hydrocarbons, benzene, toluene, acetone, and tetrahydrofuran. Hexane solutions of **1** exhibit an intense infrared absorption at 1685 cm^{-1} characteristic of a triply bridging carbonyl group. This band, well-separated from absorption bands arising from other components of the reaction mixture, is most useful for an assessment of the relative success of the synthesis.

(b) Mass Spectral Data. Mass spectral measurements were performed with an AEI MS 902-C spectrometer on two samples of **1**. Both spectra exhibited a sufficiently large parent ion peak such that a peak match was obtained (638.1412; $esd\ 3 \times 10^{-4}$). The observed fragmentation patterns for both spectra were reasonably similar and to a large extent corresponded to the mass spectral pattern reported¹¹ for the $Co_2(\eta^5-C_5Me_5)_2(\mu_2-CO)_2$ dimer.

(c) Electrochemical Data. Cyclic voltammetric measurements were performed with a Bioanalytical Systems Electrochemical Analyzer equipped with a PAR electrochemical cell which was operated inside a Vacuum Atmospheres drybox under an atmosphere of recirculating purified nitrogen. The configuration of the cell consisted of three electrodes, viz., the working electrode which was either a glassy carbon or platinum disk, a platinum wire counter electrode, and a saturated calomel electrode (SCE) as a reference. The supporting electrolyte, tetra-*n*-butylammonium hexafluorophosphate (TBAH), was prepared via a published method,³⁰ recrystallized from absolute ethanol, and oven-dried before use.

(23) Schilling, B. E. R.; Hoffmann, R. *J. Am. Chem. Soc.* **1979**, *101*, 3456–3467.

(24) Pinhas, A. R.; Albright, T. A.; Hofmann, P.; Hoffmann, R. *Helv. Chim. Acta* **1980**, *63*, 29–49.

(25) Rausch, M. D.; Genetti, R. A. *J. Org. Chem.* **1970**, *35*, 3883–3897.

(26) Kohl, F. X.; Jutzli, P. *J. Organomet. Chem.* **1983**, *243*, 119–121.

(27) Roe, D. M.; Maitlis, P. M. *J. Chem. Soc. (A)*, **1971**, 3173–3175.

(28) Huang, J.-S.; Cirjak, L. M.; Dahl, L. F., unpublished results.

(29) Beevor, R. G.; Frith, S. A.; Spencer, J. L. *J. Organomet. Chem.* **1981**, *221*, C25–C27.

(30) Lange, W.; Müller, E. *Chem. Ber.* **1930**, *63*, 1058–1070.

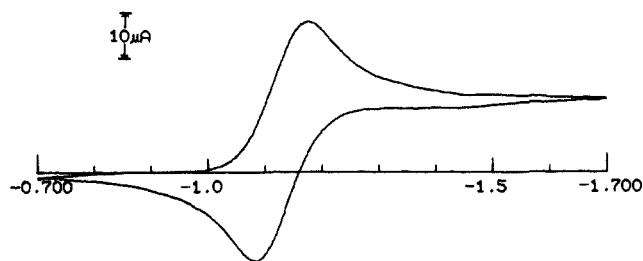


Figure 2. Cyclic voltammogram of $\text{Co}_3(\eta^5\text{-C}_5\text{Me}_5)_3(\mu_3\text{-CO})_2$ in THF/0.1 M $[\text{NBu}_4]^+[\text{PF}_6]^-$ at a platinum disk electrode with a scan rate of 10 mV/s. A reversible reduction couple is observed at $E_{1/2} = -1.13$ V (vs. SCE) with $\Delta E = 95$ mV. An assignment of this couple as a one-electron process involving the reduction of the neutral 46-electron parent to its 47-electron monoanion was made on the basis that cyclic voltammograms of equimolar solutions of **1** and two standards with reversible one-electron couples showed similar relative peak heights (within 15%) for their couples.

Supporting electrolyte concentration was maintained at 0.1 M, and iR compensation for solution resistance was made before measurement of the current vs. voltage curves.

A cyclic voltammogram of **1** is presented in Figure 2. The results of three separate experiments established that the observed reversible reduction couple for **1** involves a one-electron process. Equimolar solutions (ca. 10^{-3} M) of ferrocene, benzoquinone, and **1** were carefully prepared within a Vacuum Atmospheres drybox (which contained a microanalytical balance) from a stock solution of dry, degassed THF with a 0.1 M concentration of TBAH. The diffusion-controlled current for each of the three equimolar solutions was determined by use of a freshly polished Pt working electrode. Cyclic voltammograms obtained for the three solutions were measured within minutes of each other under a procedure designed to keep the experimental conditions of temperature, electroactive material concentration, scan rate, and electrode configuration as constant as possible. In each experiment, the measured diffusion currents for the well-characterized one-electron oxidation couple of ferrocene, the first one-electron reduction couple of benzoquinone, and the reduction couple of **1** were found to be equal within experimental error (ca. 15%).

(d) Solid-State Magnetic Susceptibility Data. Temperature- and field-dependent magnetic susceptibility studies were carried out on two samples of **1** with a SHE series 900 superconducting SQUID magnetometer (University of California—Berkeley). Each sample (the first, 10 mg; the second, 27 mg) was loaded inside a Vacuum Atmospheres drybox into a kel-f container and sealed under argon. The magnetic susceptibilities reported here have been corrected for the diamagnetism of the kel-f container; this diamagnetism was small and field dependent. Data were obtained for each sample over a temperature range of 4 to 280 K at magnetic fields from 1 to 40 kG (in order to check for ferromagnetic impurities). A small field dependence was noted for both samples. The considerably lower susceptibilities found for the second sample at low temperatures indicated that this sample was markedly more pure, in harmony with the considerably greater precautions exercised in its purification and in the handling techniques.³¹ Since the paramagnetism of the second sample was markedly less than that of the first sample, the residual paramagnetism in the second sample below 40 K is probably not intrinsic but due to some remaining impurities. An analysis of the magnetic susceptibility data is presented for only the second sample.

In order to correct for the field dependence of the second sample, magnetizations for different field strengths (10, 20, 30, and 40 kG) were measured over the temperature range of 4 to 280 K. A linear extrapolation of the field strengths to zero field for 25, 50, 100, and 280 K gave values within 0.06×10^{-3} G of the mean of 0.9×10^{-3} G for the saturation magnetization (M_s). On the basis of a M_s value of 157 G/g for cobalt metal (a possible ferromagnetic impurity), approximately 6 μg of cobalt metal (which for a 0.026-g sample corresponds to a 0.02% im-

(31) In the case of the second sample of **1**, extreme care was exercised in the purification and handling of this compound. The sample was chromatographed twice on alumina (rigorously purged with N_2 and flushed with dry degassed solvent), and all transfers of the material were made without contact with metal objects such as spatulas. As a final precaution, the sample was dissolved in dry, degassed benzene- d_6 and filtered through a glass-wool plug into a storage vessel in a Vacuum Atmospheres drybox. The solvent was removed under vacuum, and the container was hermetically sealed and placed inside another Schlenk tube under N_2 for shipment to UC—Berkeley. Proton NMR and IR spectra of this sample prior to the magnetic susceptibility measurements and an IR spectrum of the sample after the measurements did not exhibit any evidence for impurities or decomposition products.

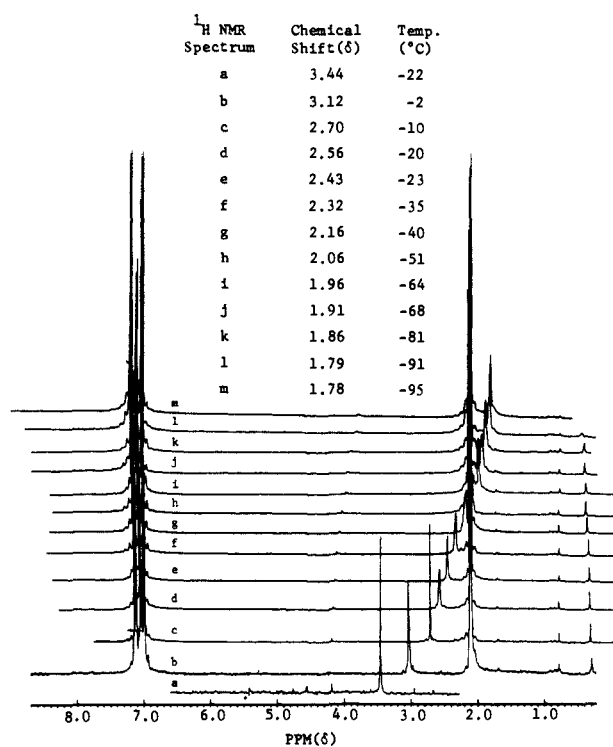


Figure 3. The isotropic-shift dependence of the methyl proton resonance on temperature displayed by variable-temperature ^1H NMR spectra of $\text{Co}_3(\eta^5\text{-C}_5\text{Me}_5)_3(\mu_3\text{-CO})_2$ (**1**) in toluene- d_8 . The observed change in chemical shift of the single methyl resonance from a paramagnetic-induced value of δ 3.44 at room temperature (22 °C) to a diamagnetic limiting value of δ 1.78 at -95 °C is ascribed to a temperature-dependent equilibrium in solution between singlet and triplet spin states for this 46-electron system. The large residual resonances at δ 2.0 and 7.1 are due primarily to $\text{C}_6\text{D}_5\text{CD}_2\text{H}$ and $\text{C}_6\text{D}_4\text{HCD}_3$ impurities (ca. 0.1%), respectively, in the toluene- d_8 solvent.

urity) will account for this field dependence.

(e) Solution Magnetic Susceptibility and Temperature-Dependent Proton NMR Data. The bulk susceptibility in a 2% cyclohexane/ C_6D_6 solution was determined at room temperature (23 °C) via the Evans method³² on a Bruker 270-MHz spectrometer; an effective magnetic moment (corrected for metal and ligand diamagnetic susceptibilities³³) of 1.4 μ_B was obtained. This value is considerably smaller than that expected for a diradical with two unpaired electrons.

A room-temperature ^1H NMR spectrum of **1** on a Bruker WP-270 spectrometer exhibited a sharp singlet at δ 3.45 (benzene- d_6). The occurrence of this proton methyl resonance at a much lower field than the δ 1.2–2.0 ppm range normally observed for methyl proton signals in diamagnetic metal pentamethylcyclopentadienyl complexes is readily ascribed to the paramagnetic nature of **1**. A subsequent study with the Bruker WP-270 spectrometer of the ^1H NMR spectra of **1** in toluene- d_8 at different temperatures revealed a dramatic temperature dependence of the methyl proton resonance for the three equivalent pentamethylcyclopentadienyl rings (Figure 3). At low temperature (ca. -95 °C) a normal unshifted resonance at δ 1.78 (corresponding to a diamagnetic limiting value) was observed. As the sample was heated, a gradual shift to lower fields occurred such that at +97 °C the observed ^1H resonance was δ 5.60. This behavior is characteristic of an isotropic shift arising from a singlet-triplet equilibrium (vide infra).

(f) Crystal Structure. Crystals of **1** (mol wt 638.5) suitable for X-ray analysis were obtained from a slow cooling of a hexane solution under nitrogen. A parallelepiped-shaped black crystal (of approximate dimensions 0.35 \times 0.40 \times 0.60 mm) was mounted under an argon atmosphere inside a Lindemann glass capillary which was then hermetically sealed. X-ray diffraction measurements were made at ambient tem-

(32) (a) Evans, D. F. *Proc. Chem. Soc.* **1958**, 115–116. (b) Evans, D. F. *J. Chem. Soc.* **1959**, 2003–2005. (c) Fritz, H. P.; Schwarzhan, K.-E. *J. Organomet. Chem.* **1964**, *1*, 208–211. (d) Live, D. H.; Chan, S. I. *Anal. Chem.* **1970**, *42*, 791–792. (e) Ostfeld, D.; Cohen, I. A. *J. Chem. Educ.* **1972**, *49*, 829. (f) Gerger, W.; Mayer, U.; Gutmann, V. *Monatsh. Chem.* **1977**, *108*, 417–422.

(33) Drago, R. S. *Physical Methods in Chemistry*; W. B. Saunders, 1977; p 413.

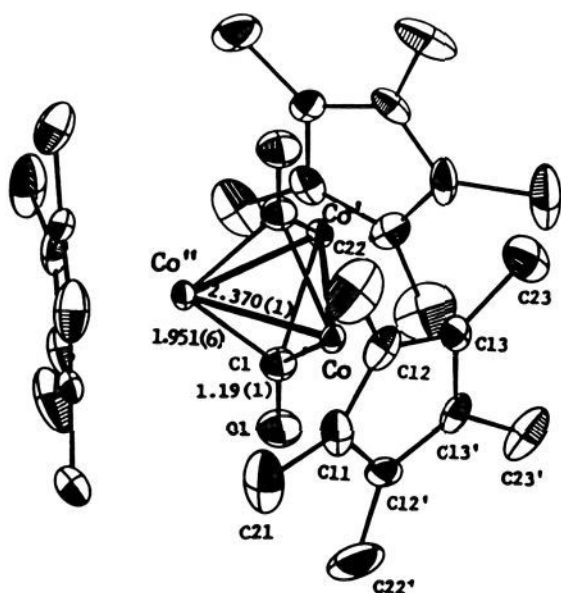


Figure 4. Molecular configuration and atom-labeling scheme for $\text{Co}_3(\eta^5\text{-C}_5\text{Me}_5)_3(\mu_3\text{-CO})_2$ (**1**) which possesses crystallographic $C_{3h}\text{-}3/m$ site symmetry. The anisotropic thermal ellipsoids for all non-hydrogen atoms are drawn at the 20% probability level. The normal sizes, shapes, and orientations of the atomic thermal ellipsoids for the $\text{Co}_3(\text{CO})_2$ core provide no evidence that this configuration is an "averaged" threefold-disordered structure involving the superposition of an "instantaneous" geometry which is considerably distorted from $C_{3h}\text{-}3/m$ symmetry.

perature (22 °C) on a Syntex (Nicolet) P1 diffractometer with graphite-monochromatized Mo K α radiation. Details of crystal alignment and data collection parameters along with a listing of crystallographic programs used are given elsewhere.³⁴ A hexagonal unit cell with dimensions $a = b = 10.636$ (3) Å and $c = 15.294$ (7) Å (determined from 15 well-centered high-angle reflections) was chosen; axial photographs, which verified the lattice lengths, corresponded to $C_{6h}\text{-}6/m$ Laue symmetry. The calculated density for $V = 1498$ (1) Å³ and $Z = 2$ is 1.39 g/cm³.

Intensities for two octants ($+h, \pm k, l$) were measured via the $\theta\text{-}2\theta$ scan mode over a 2θ range of 3.0 to 45.0° with variable scan speeds of 3.0–24.0 deg/min and scan widths of 1° below 2θ ($K\alpha_1$) to 1° above 2θ ($K\alpha_2$).

Two standard reflections, which were recollected after every 50 measured intensities, showed less than 3% variations in their intensities over the course of data acquisition. The data were corrected for absorption via ψ scans. Merging of the multiply observed reflections (2048) under $C_{6h}\text{-}6/m$ symmetry yielded 621 independently observed reflections with an unweighted $R_1(F)$ merging index of 2.7%.

Observed systematic absences of $\{00l\}$ for l odd are consistent with the probable space groups $P6_3$ and $P6_3/m$; our choice of the latter centrosymmetric space group was confirmed by the successful direct-methods solution of the crystal structure with MULTAN³⁵ and its subsequent refinement. The crystallographically independent unit consisting of one cobalt atom (lying on a mirror plane), one carbonyl ligand, and one-half a pentamethylcyclopentadienyl ring (bisected by a mirror plane) was refined with the least-squares program RAELS,³⁶ in which individual positional and anisotropic thermal parameters were varied for each non-hydrogen atom. Since reliable coordinates for the methyl hydrogen atoms were not revealed from electron-density difference maps, idealized hydrogen positions were calculated with MIRAGE³⁷ and included in the refinement via the following model. For each of the three independent methyl substituents, two twofold-related orientations of half-weighted tetrahedral-like positions with fixed isotropic temperature factors were refined in RAELS by the use of slack constraints³⁸ (involving equal and opposite change cards for the occupancy factors) to determine which of

(34) Byers, L. R.; Dahl, L. F. *Inorg. Chem.* **1980**, *19*, 277–284.

(35) Main, P.; Lessinger, L.; Woolfson, M. M.; Germain, G.; Declercq, J.-P. *MULTAN-78*, Germain, G.; Main, P.; Woolfson, M. M. *Acta Crystallogr., Sect. A* **1971**, *A27*, 368–376.

(36) Rae, A. D. *RAELS—A Comprehensive Least-Squares Program*; University of New South Wales: Kensington, 1976. Adapted for a Harris/7 computer by A. D. Rae, University of Wisconsin, Madison, 1983.

(37) Calabrese, J. C., *MIRAGE*, Ph.D. Thesis, University of Wisconsin—Wisconsin, 1971, Appendix III.

(38) Rae, A. D. *Acta Crystallogr.* **1975**, *A31* 570–574.

Table I. Positional Parameters for $\text{Co}_3(\eta^5\text{-C}_5\text{Me}_5)_3(\mu_3\text{-CO})_2$

no.	atom	x	y	z
1	Co	0.216 71 (8)	−0.311 99 (8)	0.750 00 (0)
2	O1	0.333 33 (0)	−0.333 33 (0)	0.918 94 (41)
3	C1	0.333 33 (0)	−0.333 33 (0)	0.841 06 (57)
4	C13	0.004 63 (45)	−0.392 69 (51)	0.798 29 (32)
5	C12	0.090 33 (53)	−0.250 49 (61)	0.825 17 (36)
6	C11	0.143 98 (82)	−0.159 82 (77)	0.750 00 (0)
7	C23	−0.080 18 (64)	−0.515 87 (74)	0.855 53 (50)
8	C22	−0.120 87 (84)	−0.192 37 (99)	0.913 75 (56)
9	C21	0.219 92 (108)	0.002 52 (91)	0.750 00 (0)

Table II. Intramolecular Distances and Bond Angles for $\text{Co}_3(\eta^5\text{-C}_5\text{Me}_5)_3(\mu_3\text{-CO})_2$ Occupying a $C_{3h}\text{-}3/m$ Symmetry Site

A. Bond Lengths (Å)			
Co–Co	2.370 (1)	C11–C12	1.424 (7)
Co–C1	1.951 (6)	C12–C13	1.382 (7)
Co–C11	2.114 (7)	C13–C13'	1.477 (10)
Co–C12	2.106 (4)	C11–C21	1.496 (11)
Co–C13	2.106 (4)	C12–C22	1.457 (9)
		C13–C23	1.454 (7)
B. Bond Angles (deg)			
C1–O1	1.190 (10)	C12–C11–C12'	107.7 (6)
C1–C1	2.785 (17)	C12–C11–C21	125.7 (3)
Co–O1	2.924 (6)	C13–C12–C11	108.8 (5)
		C13–C12–C22	128.8 (6)
Co–Cp(cent.)	1.73	C12–C13–C13'	107.3 (3)
		C12–C13–C23	125.4 (6)

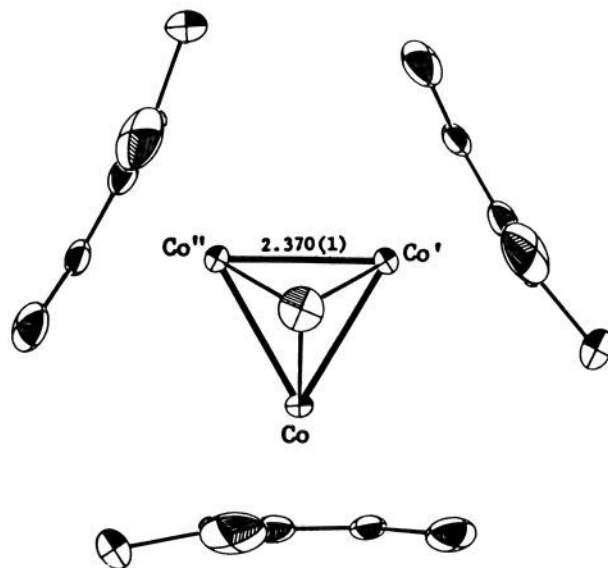


Figure 5. View down the principal threefold axis of $\text{Co}_3(\eta^5\text{-C}_5\text{Me}_5)_3(\mu_3\text{-CO})_2$ (**1**) which conforms to crystallographically imposed $C_{3h}\text{-}3/m$ site symmetry. The gear-like arrangement of the nearest inter-ring methyl substituents in the sterically crowded crystal-ordered C_5Me_5 rings is apparent.

the twofold-related methyl hydrogen orientations was preferred. Full-matrix least-squares refinement of the model converged at $R_1(F) = 3.78\%$ and $R_2(F) = 5.73\%$ with the maximum parameter shift-to-error ratio (Δ/σ) being 0.01; the goodness-of-fit value was 2.76, and the data (m)-to-parameter (n) ratio was 10.5/1.^{39,40}

(39) The unweighted and weighted discrepancy factors used are $R_1(F) = [\sum ||F_o| - |F_c|| / \sum |F_o|] \times 100$ and $R_2(F) = [\sum w_i ||F_o| - |F_c||^2 / \sum w_i |F_o|^2]^{1/2} \times 100$. All least-squares refinements were based on the minimization of $\sum w_i ||F_o| - |F_c||^2$ with individual weights of $w_i = 1/\sigma^2(F_o)$ assigned on the basis of the estimated standard deviations of the observed structure factors. The standard deviation in an observation of unit weight ("goodness-of-fit") is defined by $[\sum w_i (|F_o| - |F_c|)^2 / (m - n)]^{1/2}$.

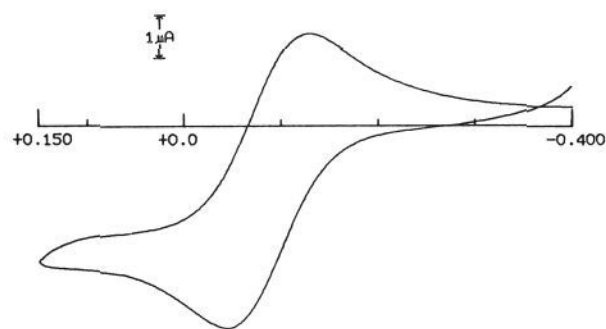


Figure 6. Cyclic voltammogram of the 48-electron $\text{Co}_3(\eta^5\text{-C}_5\text{Me}_5)_3(\mu_3\text{-CO})(\mu_3\text{-O})$ in $\text{CH}_2\text{Cl}_2/0.1 \text{ M } [\text{NBu}_4]^+[\text{PF}_6]^-$ at a platinum disk electrode with a scan rate of 15 mV/s. A reversible oxidation couple is indicated at $E_{1/2} = -0.09 \text{ V}$ (vs. SCE) with $\Delta E = 82 \text{ mV}$.

Since the refined occupancy factors for the three independent sets of methyl hydrogen positions converged to equally weighted values, the refinement did not indicate a preferred orientation of the methyl hydrogen atoms for the three independent methyl groups in the mirror-bisected pentamethylcyclopentadienyl ring. A final electron-density difference map did not exhibit any unusual features. Atomic positional parameters for the non-hydrogen atoms from the last cycle of least-squares refinement are given in Table I, while selected interatomic distances and angles are given in Table II. Calculated coordinates and isotropic temperature factors for all hydrogen atoms, anisotropic thermal parameters for all non-hydrogen atoms, and a listing of observed and calculated structure factor amplitudes are available as supplementary material. Each of the molecular configurations (Figures 4 and 5) was computer-drawn with ORTEP II.⁴¹

Characterization of $\text{Co}_3(\eta^5\text{-C}_5\text{Me}_5)_3(\mu_3\text{-CO})(\mu_3\text{-O})$ (3). (a) **Properties and Infrared Data.** This compound, isolated in very low yield (vide supra), is a black crystalline solid which is soluble in a variety of organic solvents such as hexane, benzene, toluene, dichloromethane, and acetone. Solution infrared spectra exhibit a strong carbonyl absorption band at 1665 cm^{-1} , and likewise a KBr-pellet spectrum gives a strong band at 1660 cm^{-1} .

(b) **Mass Spectral Data.** The composition of 3 was unequivocally established from mass spectral measurements by Dr. R. B. Cody (Nicolet Analytical Instruments) on a Nicolet FT MS-1000 mass spectrometer. Ionization by electron impact provided a positive ion mass spectrum (IP = 13 eV, inlet temperature = $238 \text{ }^\circ\text{C}$) for 3 from which the parent ion peak was observed with the second highest intensity (at 89% relative to the highest base intensity for the $[\text{Co}(\text{C}_5\text{Me}_5)_2]^+$ peak at m/e 329). A peak matching of the parent ion peak corresponding to an exact mass of 626.1375 vs. a calculated value of 626.1404 for the formula of 3. A negative ion mass spectrum (IP = 13 eV, inlet temperature = $178 \text{ }^\circ\text{C}$) of 3 showed the highest base intensity to correspond to the parent ion peak at m/e 626.

(c) **Proton NMR Data.** A ^1H NMR spectrum of 3 at room temperature on a Bruker WP-270 spectrometer showed a sharp singlet in acetone- d_6 at δ 1.64 which was assigned to the equivalent methyl protons for the three C_5Me_5 rings. No other proton resonances were detected (besides that for acetone- d_5 impurity) within a sweep width of 12000 Hz.

(d) **Electrochemical Data.** Cyclic voltammetric measurements, obtained as previously described for 1, were made on ca. 10^{-3} M solutions of 3 in dichloromethane. A single oxidation couple was observed (Figure 6) at an $E_{1/2}$ value of -0.09 V (vs. SCE) with a peak-to-peak separation of 82 mV for a scan rate of 15 mV/s. Evidence for the couple being reversible is given by the anodic and cathodic currents being approximately equal at this slow scan rate; however, at faster rates the peak currents were no longer comparable (e.g., at 100 mV/s, $|i_a|$ is differed from $|i_c|$ by ca. 10%) thereby indicating that a kinetically slow electron transfer may be occurring. No attempt was made to determine by a comparative analysis of measured diffusion currents for 3 and a known standard whether the above couple involves a one- or two-electron oxidation process.

Preparation and Characterization of $\text{Rh}_3(\eta^5\text{-C}_5\text{Me}_5)_3(\mu_3\text{-CO})_2$ (2). A solution of 0.5 g (1.1 mmol) of $\text{Co}_2(\eta^5\text{-C}_5\text{Me}_5)_2(\mu_2\text{-CO})_2$ and 0.43 g (0.8

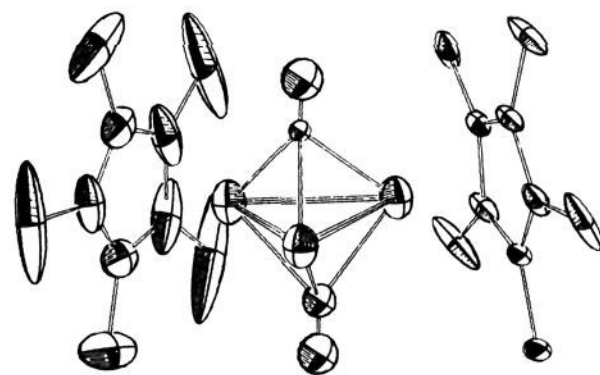


Figure 7. The "averaged" structure of $\text{Rh}_3(\eta^5\text{-C}_5\text{Me}_5)_3(\mu_3\text{-CO})_2$ (determined at room temperature) which has a crystallographic vertical mirror plane passing through one rhodium atom (on the left) and both carbonyl ligands. Only one of the two mirror-plane-related orientations of the crystallographically disordered and (rigid-body)-refined C_5Me_5 ring possessing the unusually large carbon thermal ellipsoids is shown; likewise, one of the other two mirror-related C_5Me_5 rings is omitted for the purpose of clarity. The abnormal sizes, shapes, and orientations of the atomic thermal ellipsoids for both the $\text{Rh}_3(\text{CO})_2$ core and C_5Me_5 rings provide convincing evidence for a crystal-disordered averaged structure resulting from the superposition of the actual "instantaneous" configuration (whose $\text{Rh}_3(\text{CO})_2$ core is markedly distorted from an idealized D_{3h} geometry toward a C_{2v} one) found for $\text{Rh}_3(\eta^5\text{-C}_5\text{Me}_5)_3(\mu_3\text{-CO})_2$ from a low-temperature X-ray diffraction study.²⁰

mmol) of $\text{Rh}_2(\eta^5\text{-C}_5\text{Me}_5)_2(\mu_2\text{-CO})_2$ in 100 mL of hexane was prepared and then added to a water-cooled Pyrex photolysis unit under a nitrogen atmosphere. The blue-green solution was then photolyzed with a medium-pressure Hg lamp for 12 h. Infrared spectra of the solution after 12 h indicated an extremely complex reaction mixture. The solvent was reduced in volume, and purification was attempted by careful chromatography on alumina. The fractions collected (in order of elution) consisted of the hexane-eluted light orange $\text{Co}(\eta^5\text{-C}_5\text{Me}_5)(\text{CO})_2$ followed by the hexane/toluene-eluted dark green $\text{Co}_2(\eta^5\text{-C}_5\text{Me}_5)_2(\mu_2\text{-CO})_2$ followed closely by a toluene-eluted blue band. Infrared spectra of the latter fraction displayed an absorption band at 1735 cm^{-1} characteristic of the $\text{Rh}_3(\eta^5\text{-C}_5\text{Me}_5)_3(\mu_3\text{-CO})_2$ dimer. Fractional crystallization of this band in hexane yielded a small quantity of black crystals which were identified as $\text{Rh}_3(\eta^5\text{-C}_5\text{Me}_5)_3(\mu_3\text{-CO})_2$ from a mass spectrum (that exhibited a large parent ion peak at m/e 770) obtained on an AEI MS 902-C spectrometer. The formulation of this compound as the trirhodium analogue of 1 was substantiated by an X-ray diffraction study (vide infra).

A small black parallelepiped-shaped crystal of 0.1 mm size along each direction was mounted under argon inside a Lindemann glass capillary which was evacuated, filled with argon, and then hermetically sealed. Axial photographs taken on a Syntex (Nicolet) PI diffractometer about the three principal axial directions showed the crystal to be orthorhombic. The determined lattice constants (from the centered crystal) of $a = 15.312(1) \text{ \AA}$, $b = 11.166(6) \text{ \AA}$, $c = 18.166(6) \text{ \AA}$ give rise to a calculated unit-cell volume of $3106(3) \text{ \AA}^3$. The calculated density is 1.64 g/cm^3 based on $Z = 4$. Systematic absences indicated the probable space groups to be either $Pca2_1$ or $Pcam$. The latter centrosymmetric space group requires each molecule to lie on a crystallographic mirror. Intensity data were collected at room temperature with graphite-monochromatized $\text{Mo K}\alpha$ radiation ($\lambda = 0.71073 \text{ \AA}$) via the θ - 2θ scan mode over a 2θ range of 3 - 40° . Reduction of the 3112 data obtained for two octants $\{h, k, \pm l\}$ to one independent octant yielded 639 reflections with $I \geq 2.5\sigma(I)$.

The crystal structure was solved by the application of MULTAN³⁵ and refined with the least-squares program RAELS.³⁶ The model utilized in refinements under both $Pca2_1$ and $Pcam$ symmetry used individual anisotropic thermal parameters for the rhodium and carbonyl atoms and a rigid-group constraint of each C_5Me_5 ring to a C_{5v} geometry with the thermal motion of each ring described by a TLX model.³⁸

The best least-squares refinement was achieved under $Pcam$ symmetry which resulted in a crystal disordering of the C_5Me_5 ring bisected by the crystallographically imposed mirror plane. This refinement converged at $R_1(F) = 8.6\%$, $R_2(F) = 15.2\%$, with a goodness-of-fit value of 3.7 and a data-to-parameter ratio of $8.9/1$.^{39,40}

The mirror-disordered "averaged" configuration of $\text{Rh}_3(\eta^5\text{-C}_5\text{Me}_5)_3(\mu_3\text{-CO})_2$ is clearly indicated in Figure 7. An ordered crystal structure of $\text{Rh}_3(\eta^5\text{-C}_5\text{Me}_5)_3(\mu_3\text{-CO})_2$ was independently determined at low temperature by Dr. Judith Howard (Department of Inorganic Chemistry, the University of Bristol, Great Britain), who graciously supplied a molecular

(40) Atomic scattering factors including anomalous dispersion corrections were taken from the following: *International Tables for X-Ray Crystallography*; Kynoch: Birmingham, England, 1974; Vol. IV, p 149, pp 155-157.

(41) Johnson, C. K., *ORTEP-II, A FORTRAN Thermal-Ellipsoid Plot Program for Crystal Structure Illustrations*; ORNL-5138, Oak Ridge National Laboratory, Oak Ridge, TN, 1976.

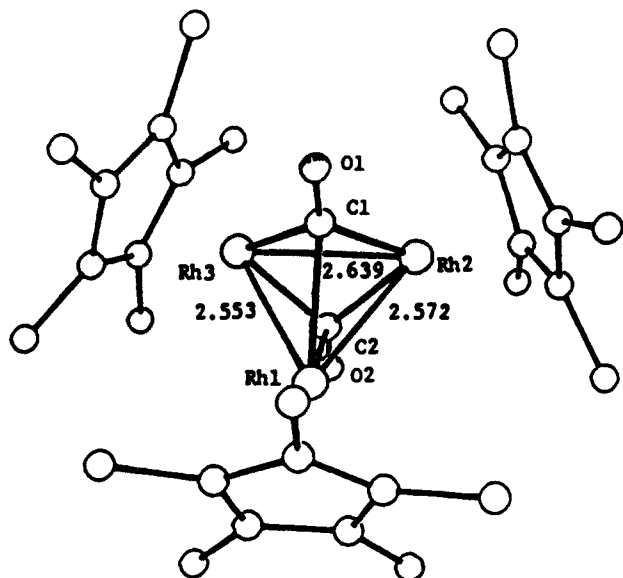


Figure 8. The actual molecular configuration of the crystal-ordered $\text{Rh}_3(\eta^5\text{-C}_5\text{Me}_5)_3(\mu_3\text{-CO})_2$, prepared by Stone and co-workers¹⁹ and obtained from a low-temperature X-ray diffraction study by Howard.^{20a} The dimensions reveal a distinct distortion of the entire $\text{Rh}_3(\text{CO})_2$ core of crystallographic C_1 —1 site symmetry from an idealized D_{3h} geometry toward a C_{2v} one with *one* long and *two* short Rh—Rh bonds (2.639 (2) Å vs. 2.562 Å (av)) and with *two* long and *four* short Rh—CO bonds (2.345 Å (av) vs. 1.985 Å (av)).

drawing (Figure 8) with selected distances.

A comparison of the low-temperature orthorhombic lattice dimensions with those given above showed good agreement for the *a* and *c* lengths but revealed that the *b* axis obtained in the low-temperature study was twice that given above. It is also noteworthy that a doubling of the above axis to a value of 22.32 Å will give rise to a *b* glide in the *c* direction, which in turn gives rise to the probable space group of *Pcab* in accordance with that found by Howard.^{20a} Since a reexamination of our axial photographs about the *b* axis taken at room temperature did not indicate any weak reflections indicative of a doubled *b* axis, it is presumed that the particular (weakly diffracting) crystal examined in our laboratories was either disordered (at room temperature) or the *k* odd reflections were simply not detected under our experimental conditions. When it was learned that Stone and co-workers¹⁹ had independently obtained this compound and that Howard^{20a} had precisely determined its structure, we terminated further work.

Results and Discussion

Synthesis and Spectral-Electrochemical Properties of $\text{Co}_3(\eta^5\text{-C}_5\text{Me}_5)_3(\mu_3\text{-CO})_2$ (1) and $\text{Co}_3(\eta^5\text{-C}_5\text{Me}_5)_3(\mu_3\text{-CO})(\mu_3\text{-O})$ (3). The original isolation of **1** occurred during an unsuccessful attempt to prepare the unknown iron-dicobalt cluster, $\text{Me}(\eta^5\text{-C}_5\text{H}_5)\text{-FeCo}_2(\eta^5\text{-C}_5\text{Me}_5)_2(\mu_2\text{-CO})_2(\mu_3\text{-CO})$, by a photochemical reaction of $\text{Co}_2(\eta^5\text{-C}_5\text{Me}_5)_2(\mu_2\text{-CO})_2$ and $\text{Fe}(\eta^5\text{-C}_5\text{H}_5)(\text{CO})_2\text{Me}$. This reaction unexpectedly produced the dark-brown **1** as a low-yield side product. Repeated attempts to prepare **1** either photochemically or thermally by the rational synthetic route of $\text{Co}_2(\eta^5\text{-C}_5\text{Me}_5)_2(\mu_2\text{-CO})_2$ and $\text{Co}(\eta^5\text{-C}_5\text{Me}_5)(\text{C}_2\text{H}_4)_2$ failed. Subsequent preparations of **1** were accomplished by photolytic decomposition of $\text{Co}(\eta^5\text{-C}_5\text{Me}_5)(\text{CO})_2$ which, in addition to $\text{Co}_2(\eta^5\text{-C}_5\text{Me}_5)_2(\mu_2\text{-CO})_2$ as the major product, gives both **1** and **3** in very low yields (1–2%).

The composition of **1** was conclusively determined from high-resolution mass spectra which exhibited the parent ion peak and from an X-ray diffraction analysis. A fingerprinting identification of **1** is provided from infrared spectra which display a strong carbonyl absorption band at 1685 cm^{-1} . This highly air-sensitive compound is soluble in common solvents. A cyclic voltammogram (Figure 2) of **1** in tetrahydrofuran solution exhibited one 0/–1 reduction couple at an $E_{1/2}$ value of -1.13 V (vs. SCE) with a peak-to-peak separation of 95 mV for a scan rate of 10 mV/s. Evidence for its reversible nature is given by the anodic and cathodic peak currents being essentially equal for a given scan

rate. Attempts to observe a second reduction couple for **1** to its presumed dianion (by scanning to a cathodic limit of -2.2 V in THF) were unsuccessful. In view of **1** being electronically unsaturated, it is somewhat surprising that preliminary efforts to add molecular hydrogen and carbon monoxide to **1** were unsuccessful.

The black crystalline **3** is a pentamethylcyclopentadienyl analogue of $\text{Co}_3(\eta^5\text{-C}_5\text{H}_5)_3(\mu_3\text{-CO})(\mu_3\text{-O})$.⁴² Its stoichiometry was unambiguously established from high-resolution mass spectra which showed the parent ion peak. This compound is also soluble in a large variety of organic solvents. Solution infrared spectra of **3** display a strong carbonyl band at 1665 cm^{-1} . The expected diamagnetism for this 48-electron cluster is in accordance with a ^1H NMR spectrum (acetone-*d*₆) exhibiting a sharp singlet within the normal methyl proton range. A cyclic voltammogram (Figure 6) shows a single reversible oxidation couple.

Crystal and Molecular Structure of $\text{Co}_3(\eta^5\text{-C}_5\text{Me}_5)_3(\mu_3\text{-CO})_2$ (1). (a) **Overall Description.** Tris(pentamethylcyclopentadienyl)tricobalt dicarbonyl exists in the solid state as discrete molecules with no unusual intermolecular contacts. This 46-electron cluster (Figure 4) is composed of an equilateral triangle of $\text{Co}(\text{C}_5\text{Me}_5)$ fragments that are linked to one another by the two triply bridging carbonyl ligands as well as direct Co—Co interactions. The resulting configuration of crystallographic C_{3h} — $3/m$ site symmetry is similar to those of the well-known Fischer—Palm 49-electron $\text{Ni}_3(\eta^5\text{-C}_5\text{H}_5)_3(\mu_3\text{-CO})_2$ molecule^{43,44} and the corresponding pentamethylcyclopentadienyl analogue.⁴⁵

Two views of **1** showing the anisotropic thermal ellipsoids for all non-hydrogen atoms are given in Figures 4 and 5. The fact that a temperature-dependent magnetic susceptibility analysis established that **1** does not have two unpaired electrons in the solid state necessitates that **1** possess a molecular distortion from threefold symmetry which would break the degeneracy of the half-filled e'' HOMO (under D_{3h} symmetry). However, an examination of the sizes, shapes, and orientations of the atomic thermal ellipsoids in Figures 4 and 5 as well as their root-mean-square displacements does not indicate any abnormalities. In particular, the isotropic nature of the thermal ellipsoids for the cobalt and carbonyl carbon atoms makes it appear unlikely that the determined configuration represents an “averaged” threefold-disordered superposition of a *substantially distorted* $\text{Co}_3(\text{CO})_2$ core possessing either C_{2v} or C_s symmetry.

Attempts to lower the molecular C_{3h} — $3/m$ site symmetry of the crystal lattice by a slow cooling of the crystal to $-80\text{ }^\circ\text{C}$ were unsuccessful. X-ray diffraction data showed that the unit cell remained hexagonal throughout the cooling process and all symmetry-related pairs of reflections which were collected gave good intensity agreement.

(b) **Cobalt—Cobalt Distances.** The Co—Co bond length for the three symmetry-equivalent distances is only 2.370 (1) Å. In order to provide an operational test that this relatively short Co—Co distance in **1** is indicative of tricobalt multiple-bond character, the 48-electron $[\text{Co}_3(\eta^6\text{-C}_6\text{H}_6)_3(\mu_3\text{-CO})_2]^+$ monocation, whose preparation and IR spectrum had been reported⁴⁶ in 1958, was spectroscopically and structurally analyzed.⁴⁷ A comparative analysis revealed that the mean Co—Co bond-length difference of 0.029 Å between the 46-electron **1** and the closely related 48-electron cobalt benzene trimer containing the same $\text{Co}_3(\text{CO})_2$ core is indeed electronically induced. The significantly larger Co—Co distance in the 48-electron $[\text{Co}_3(\eta^6\text{-C}_6\text{H}_6)_3(\mu_3\text{-CO})_2]^+$

(42) Uchtman, V. A.; Dahl, L. F. *J. Am. Chem. Soc.* **1969**, *91*, 3763–3769.

(43) Hoek, A. A.; Mills, O. S. In *Advances in the Chemistry of Coordination Compounds*; Kirschner, S., Ed.; Macmillan: New York, 1961; pp 640–648.

(44) Byers, L. R.; Uchtman, V. A.; Dahl, L. F. *J. Am. Chem. Soc.* **1981**, *103*, 1942–1951.

(45) Maj, J. J.; Rae, A. D.; Dahl, L. F. *J. Am. Chem. Soc.* **1982**, *104*, 3054–3063.

(46) (a) Chini, P.; Ercoli, R. *Gaz. Chim. Ital.* **1958**, *88*, 1170–1182. (b) Fischer, E. O.; Beckert, O. *Angew. Chem.* **1958**, *70*, 744.

(47) Olson, W. L.; Dahl, L. F. *J. Am. Chem. Soc.*, following paper in this issue.

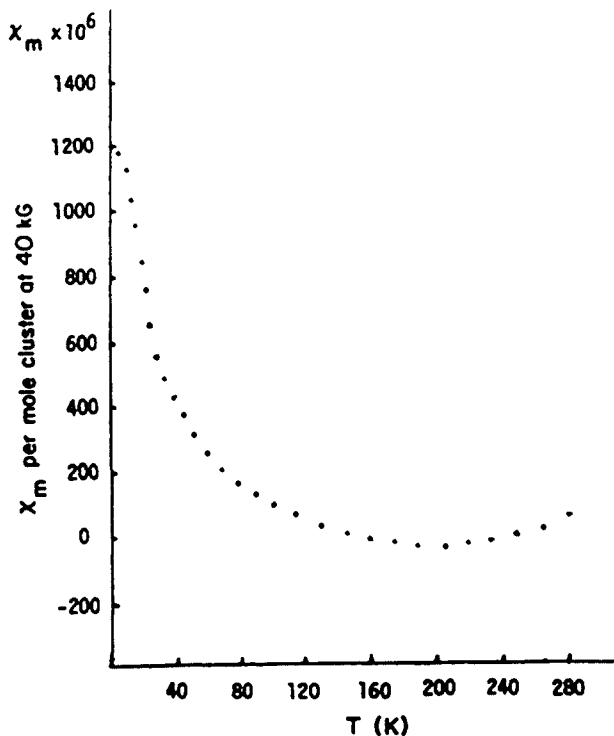


Figure 9. Temperature dependence (over a 4 to 280 K range) of the molar magnetic susceptibility at 40 kG for $\text{Co}_3(\eta^5\text{-C}_5\text{Me}_5)_3(\mu_3\text{-CO})_2$ (**1**). The χ_M values were corrected for a small ferromagnetization due to a trace impurity (ascribed to 0.02% cobalt metal) and for the diamagnetism of the kel-f container. The small Curie tail at lower temperatures indicates that trace amounts of paramagnetic impurity are present. The χ_M values show that $\text{Co}_3(\eta^5\text{-C}_5\text{Me}_5)_3(\mu_3\text{-CO})_2$ does *not* have two unpaired electrons in the solid state.

monocation is also consistent with MO calculations^{14,24,47} which showed that the half-occupied e'' HOMOs (under D_{3h} symmetry) in **1** and the corresponding completely filled e'' HOMOs in the cobalt benzene trimer possess considerable tricobalt antibonding character (see Figure 1).

(c) Distances Involving the Pentamethylcyclopentadienyl Rings. The three independent Co–C(ring) distances which range from 2.106 (4) to 2.114 (7) Å are normal and give excellent agreement with similar distances determined for $\text{Co}(\eta^5\text{-C}_5\text{Me}_5)(\text{CO})_2$ (2.062 (4)–2.105 (4) Å),³⁴ $(\eta^5\text{-C}_5\text{Me}_5)\text{CoNi}_2(\eta^5\text{-C}_5\text{H}_5)_2(\mu_3\text{-CO})_2$ (2.079 (12)–2.118 (12) Å),⁴⁴ and $\text{Co}_2(\eta^5\text{-C}_5\text{Me}_5)_2(\mu_2\text{-CO})_2$ (2.046 (11)–2.126 (11) Å).¹¹ The marked deviation of certain methyl carbon atoms in the C_5Me_5 rings from planarity (evident in Figure 5) is indicative of varying intramolecular steric effects which depend upon the orientations of the C_5Me_5 ligands relative to one another. The out-of-plane distances, which vary by 0.23, 0.05, and 0.12 Å for the C21, C22, and C23 atoms, respectively, are consistent with our expectation that the methyl groups closest to the plane of the tricobalt atoms should encounter the greatest steric interactions and therefore exhibit the largest deviations. The methyl C21 lying on the horizontal mirror plane was found to be bent out of the plane of the ring carbon atoms by 9° from the cobalt atom, while the methyl C22 and C23 atoms exhibit out-of-plane angles of 2° and 5°, respectively. These deformation angles are comparable to those previously observed for the closely related pentamethylcyclopentadienyl nickel analogue, $\text{Ni}_3(\eta^5\text{-C}_5\text{Me}_5)_3(\mu_3\text{-CO})_2$,⁴⁵ for which the analogous angles are 9°, 2°, and 2°, respectively.

The three independent C–C ring distances in the mirror-bisected C_5Me_5 ligand exhibit significant distortions from cylindrical fivefold symmetry (viz., 1.424 (7) Å for the C11–C12 bond, 1.382 (7) Å for the C12–C13 bond, and 1.477 (10) Å for the C13–C13' bond).

(d) Distances Involving the Carbonyl Ligands. The six symmetry-equivalent Co–CO and two symmetry-equivalent C–O bond lengths of 1.951 (6) and 1.190 (10) Å, respectively, are normal

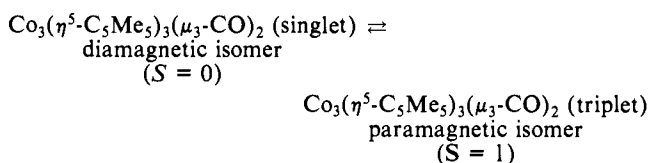
for triply bridging carbonyl ligands.

Solid-State Magnetic Susceptibility Study of $\text{Co}_3(\eta^5\text{-C}_5\text{Me}_5)_3(\mu_3\text{-CO})_2$ (1**) and Resulting Implications.** Figure 9 shows the temperature dependence of the molar magnetic susceptibility, χ_M (corrected for the field-dependent impurity), per mole of cluster measured at 40 kG. These data reveal that **1** in the solid state does not have two unpaired electrons as predicted by theory (under assumed threefold symmetry). The small Curie tail indicates that trace amounts of paramagnetic substances are also present.⁴⁸ The small positive value of $+50 \times 10^{-6} \text{ cm}^3/\text{mol}$ determined for χ_M at 280 K gradually decreases to a broad minimum which at 200 K possesses a value of $-40 \times 10^{-6} \text{ cm}^3/\text{mol}$. Correction of the χ_M values for diamagnetic contributions³³ of the cobalt and ligand atoms (viz., $\chi_M^{\text{dia}} = -371 \times 10^{-6} \text{ cm}^3/\text{mol}$) gives paramagnetic χ_M^p values of 421×10^{-6} and $331 \times 10^{-6} \text{ cm}^3/\text{mol}$ at 280 and 200 K, respectively. By use of the familiar expression $\mu_{\text{eff}} = 2.83(\chi_M^p T)^{1/2}$, the calculated effective magnetic moments of this sample are 0.97 and 0.73 μ_B at 280 and 200 K, respectively; these values are considerably less than the spin-only value of 2.83 μ_B expected for a cluster containing two unpaired electrons.

The possible origin of the residual paramagnetism of this sample is intriguing. One explanation is that partial decomposition of the sample had occurred prior to the magnetic measurements. The diamagnetism of an extremely air-sensitive organometallic complex (such as **1**) is difficult to measure in that any trace paramagnetic impurities will dominate the susceptibility.

¹H NMR Study of $\text{Co}_3(\eta^5\text{-C}_5\text{Me}_5)_3(\mu_3\text{-CO})_2$ (1**) and Resulting Implications Concerning Its Magnetic Properties and Structure in Solution. (a) Experimental Evidence for Singlet–Triplet Spin Equilibrium.** The dramatic temperature dependence of the methyl proton NMR resonance of **1** shown in Figure 3 is entirely consistent with the existence in solution of a singlet–triplet spin equilibrium. The room-temperature ¹H NMR resonance of **1** at δ 3.4 was considered highly unusual. A cooling of a toluene- d_6 solution of **1** to -95°C shifted the methyl proton resonance upfield ca. 1.7 ppm. Except at high temperatures where considerable broadening of the peak was observed, the resonance remained a symmetric singlet throughout the temperature range studied (-95 to $+97^\circ\text{C}$). No evidence for the splitting of this resonance at low temperatures into a pair of singlets with a 2:1 intensity ratio indicative of an instantaneous C_{2v} geometry was detected.

The temperature dependence of the paramagnetic shift of the signal can be readily ascribed to the existence of a singlet–triplet spin equilibrium,

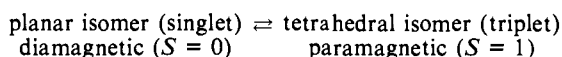


of which the singlet-state isomer is the predominant form in solution at or below room temperature. Figure 10, which displays a plot of the frequency shift of the methyl proton resonance for **1** as a function of temperature, clearly shows the nonlinear increase of the isotropic-shift magnitude with respect to the temperature.⁴⁹

(48) The measured molar magnetic susceptibility is the sum of temperature-dependent and temperature-independent (e.g., core diamagnetism) terms given by the equation $\chi_M = C/(T - \theta) + \chi_0$. For paramagnetic impurities, the molar Curie constant is small such that $C/(T - \theta)$ is of the same order of magnitude as χ_0 . Therefore, the small Curie tail below 40 K does not fit a simple Curie law (i.e., $1/T$); instead, the magnetic data must be fit to the above equation in order to obtain an accurate value of the Curie constant. It is difficult to correct accurately for both ferromagnetic and paramagnetic impurities. A ferromagnetic correction was made because it is temperature independent and therefore only shifts the magnetic data over the entire temperature range by a constant value. Since a correction for the presumed paramagnetic impurities at low temperatures would "distort" the magnetic data by changing its temperature dependence, such a correction was not made.

A similar singlet–triplet equilibrium in solution for a triangular metal cluster with two capping ligands was initially discovered⁵⁰ for the 50-electron $\text{Co}_3(\eta^5\text{-C}_5\text{H}_5)_3(\mu_3\text{-S})_2$ ^{50,51} and was recently found⁵² for the methylcyclopentadienyl-containing $\text{Co}_3(\eta^5\text{-C}_5\text{H}_4\text{Me})_3(\mu_3\text{-S})_2$ analogue.

(b) **Theoretical Treatment of the Temperature-Dependent Isotropic Behavior and Resulting Consequences.** During 1960–1970, primarily two groups, Eaton, Phillips, and colleagues⁵³ and Holm and co-workers,^{54–57} carried out extensive isotropic-shift proton NMR studies on a large number of d^8 Ni(II) bis(chelate) complexes which in noncoordinating solvents undergo configurational equilibria



This singlet–triplet equilibrium is expressed by $K_{\text{eq}} = N_t/N_s$, where N_t and N_s are the mole fractions of the triplet-state (tetrahedral) and singlet-state (planar) isomers, respectively. Their comprehensive analyses involved the use of the contact-shift equation^{55–59} to approximate the total isotropic shift of the i th proton nucleus.^{60,61}

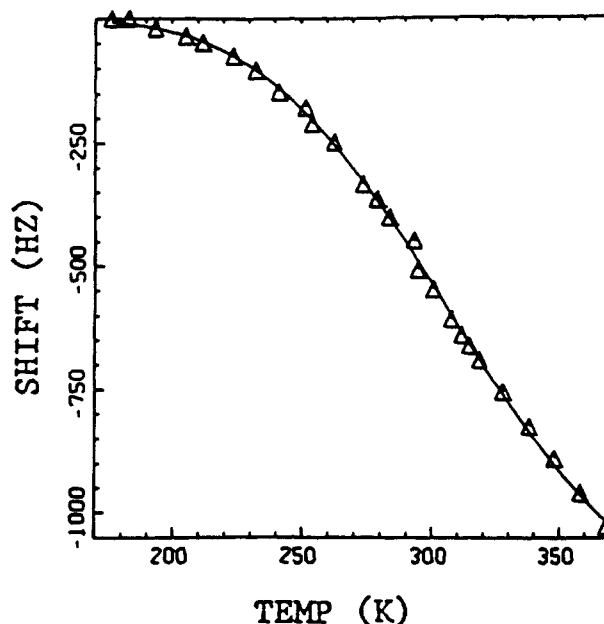


Figure 10. Plot of the frequency shift of the methyl proton resonance for the 46-electron $\text{Co}_3(\eta^5\text{-C}_5\text{Me}_5)_3(\mu_3\text{-CO})_2$ (**1**) as a function of temperature. The curve represents the “best” least-squares fit of the data points (represented by triangles) to the general form of the contact-shift equation.

(49) In the case of the paramagnetic 46-electron $(\eta^5\text{-C}_5\text{Me}_5)\text{IrCo}_2(\eta^5\text{-C}_5\text{H}_5)_2(\mu_3\text{-CO})_2$,²² room-temperature ^1H NMR spectra exhibited two upfield sharp singlets at -24.57 ($1 \text{ C}_5\text{Me}_5$) and -46.52 ($2 \text{ C}_5\text{H}_5$) ppm in an expected 3:2 intensity ratio. In complete contrast to **1**, the temperature dependence of the paramagnetic shifts of each of two proton resonances was found to be Curie-like (i.e., linear with respect to the reciprocal of temperature) over a temperature range of -93 to $+100$ °C. In addition, bulk susceptibility measurements of the IrCo_2 cluster in solution via the Evans method³² over a temperature range of -30 to $+60$ °C gave a constant magnetic moment of $\mu_{\text{eff}} = 3.36 \pm 0.4 \mu_B$. These results show that the IrCo_2 cluster in solution possesses a triplet ground state with two unpaired electrons. The fact that in the paramagnetic-shift measurements the proton signal for the two C_5H_5 ligands remained a sharp singlet down to -93 °C and showed no evidence of coalescence broadening led Herrmann et al.²² to conclude that the interconversion of the highly distorted solid-state geometry of the IrCo_2 cluster between two limiting structures (by which the two $\text{Co}(\eta^5\text{-C}_5\text{H}_5)$ fragments would be rendered equivalent on an NMR time scale) must be extremely facile and have low-energy barriers.

(50) Frisch, P. D.; Dahl, L. F. *J. Am. Chem. Soc.* **1972**, *94*, 5082–5084.

(51) (a) Sorai, M.; Kosaki, A.; Suga, H.; Seki, S.; Yoshida, T.; Otsuka, S. *Bull. Chem. Soc., Jpn.* **1971**, *44*, 2364–2371. (b) Kamijio, N.; Watanabe, T. *Acta Crystallogr.* **1979**, *B35*, 2537–2542.

(52) Pulliam, C. R.; Englert, M. H.; Dahl, L. F. *Abstracts of Papers*, 190th National Meeting of the American Chemical Society, Chicago, Illinois; American Chemical Society: Washington, DC, 1985; INOR 387.

(53) (a) Phillips, W. D.; Benson, R. E. *J. Chem. Phys.* **1960**, *33*, 607–608. (b) Benson, R. E.; Eaton, D. R.; Josey, A. D.; Phillips, W. D. *J. Am. Chem. Soc.* **1961**, *83*, 3714–3716. (c) Eaton, D. R.; Josey, A. D.; Phillips, W. D.; Benson, R. E. *J. Chem. Phys.* **1962**, *37*, 347–360. (d) Eaton, D. R.; Josey, A. D.; Phillips, W. D.; Benson, R. E., *Discuss. Faraday Soc.*, **1962**, *34*, 77–87. (e) Eaton, D. R.; Josey, A. D.; Benson, R. E.; Phillips, W. D.; Cairns, T. L. *J. Am. Chem. Soc.* **1962**, *84*, 4100–4106. (f) Eaton, D. R.; Phillips, W. D.; Caldwell, D. J. *J. Am. Chem. Soc.* **1963**, *85*, 397–406. (g) Eaton, D. R.; Josey, A. D.; Benson, R. E. *J. Am. Chem. Soc.* **1967**, *89*, 4040–4050.

(54) (a) Holm, R. H.; Swaminathan, K. *Inorg. Chem.* **1963**, *2*, 181–186. (b) Holm, R. H.; Chakravorty, A.; Dudek, G. O. *J. Am. Chem. Soc.* **1963**, *85*, 821–822. (c) Holm, R. H.; Chakravorty, A.; Dudek, G. O. *J. Am. Chem. Soc.* **1964**, *86*, 379–387. (d) Chakravorty, A.; Holm, R. H. *Inorg. Chem.* **1964**, *3*, 1010–1015. (e) Chakravorty, A.; Holm, R. H. *J. Am. Chem. Soc.* **1964**, *86*, 3999–4004. (f) Everett, E. W., Jr.; Holm, R. H. *J. Am. Chem. Soc.* **1965**, *87*, 2117–2127. (g) Holm, R. H.; Chakravorty, A.; Theriot, L. J. *Inorg. Chem.* **1966**, *5*, 625–635. (h) Ernst, R. E.; O’Connor, M. J.; Holm, R. H. *J. Am. Chem. Soc.* **1967**, *89*, 6104–6113. (i) Ernst, R. E.; O’Connor, M. J.; Holm, R. H. *J. Am. Chem. Soc.* **1968**, *90*, 5735–5744. (j) Everett, E. W., Jr.; Holm, R. H. *Inorg. Chem.* **1968**, *7*, 776–785. (k) Gerlach, D. H.; Holm, R. H. *J. Am. Chem. Soc.* **1969**, *91*, 3457–3467. (l) Powers, C. R.; Everett, E. W., Jr. *J. Am. Chem. Soc.* **1969**, *91*, 3468–3476. (m) Pignolet, L. H.; Horrocks, W. DeW.; Holm, R. H. *J. Am. Chem. Soc.* **1970**, *92*, 1855–1863.

(55) Holm, R. H. *Acc. Chem. Res.* **1969**, *2*, 307–316 and references cited therein.

(56) Holm, R. H.; O’Connor, M. J. *Prog. Inorg. Chem.* **1971**, *14*, 241–401 and references therein.

(57) Holm, R. H.; Hawkins, C. J. In *NMR of Paramagnetic Molecules: Principles and Applications*; LaMar, G. N., Horrocks, W. DeW., Jr., Eds., Academic: New York, 1973; pp 243–332.

(58) Horrocks, W. DeW., Jr. *J. Am. Chem. Soc.* **1965**, *87*, 3779–3780.

(59) Eaton, D. R.; Phillips, W. D. *Adv. Magn. Reson.* **1965**, *1*, 103–149.

The Fermi contact hyperfine interaction arises either from electron spin delocalization via symmetry-allowed mixing of spin-containing metal orbitals with ligand orbitals or from spin polarization of metal–ligand bonding orbitals by unpaired spin in metal orbitals of different symmetry; this contact shift is expressed by the relationship^{62,63} $(\Delta H_i/H_0)_{\text{contact}} = (\Delta\gamma_i/\gamma_0)_{\text{contact}} = -A_i(\gamma_e/\gamma_H)(g\beta S(S+1)/6S_kT)[\exp(\Delta G/RT) + 1]^{-1}$. In this equation, $\Delta\gamma_i$ is the frequency shift (in hertz) of the i th proton nucleus, γ_0 is the frequency of the ^1H NMR spectrometer, A_i is the isotropic hyperfine coupling constant for the i th proton, γ_e and γ_H are the gyromagnetic ratios of the electron and proton, g is the average spectroscopic splitting factor for the paramagnetic isomer, S is the total electron spin, ΔG is the free energy change defined as $\Delta G = -RT \ln K_{\text{eq}}$ for the above equilibrium, and the bracketed term is readily shown⁵⁸ to be equal to the mole fraction of the triplet isomer. The use of this equation to correlate ^1H NMR isotropic-shift data with temperature variations assumes that (1) equilibrium interconversion between the two isomers is sufficiently rapid ($>10^{-3}$ – 10^{-4} sec) such that the observed isotropic shifts are averaged over both isomers, (2) the paramagnetic isomer obeys the Curie law, and (3) the (pseudocontact) nuclear–electron dipolar interactions (which occur in magnetically anisotropic complexes and which have dependence on geometry) can be neglected.

Values of ΔG at given temperatures were obtained by the Eaton–Phillips group⁵³ and by the Holm group^{54–57} via mea-

(60) For a paramagnetic isomer, the total isotropic shift, $(\Delta H_i/H_0)_{\text{total}}$ or $(\Delta\gamma_i/\gamma_0)_{\text{total}}$ of the i th proton nucleus is defined^{55–59} as the sum of the contact and dipolar (pseudo-contact) shifts: $(\Delta H_i/H_0)_{\text{total}} = (\Delta H_i/H_0)_{\text{contact}} + (\Delta H_i/H_0)_{\text{dipolar}}$; $(\Delta\gamma_i/\gamma_0)_{\text{total}} = (\Delta\gamma_i/\gamma_0)_{\text{contact}} + (\Delta\gamma_i/\gamma_0)_{\text{dipolar}}$. Our definition of the frequency shift of the i th nucleus is given by $\Delta\gamma_i = \gamma_s - \gamma_{\text{obsd}}$, where γ_{obsd} is the observed frequency and γ_s the proton resonance for the singlet-state (diamagnetic) isomer. This definition is based on the convention⁶¹ that a negative value of the paramagnetic shift $\Delta\gamma_i$ represents a shift to lower applied magnetic field at a constant spectrometer frequency. Hence, for a constant magnetic field $\Delta\gamma_i = \gamma_{\text{dia}} - \gamma_{\text{para}}$, whereas ΔH_i is always defined as $\Delta H_i = H_{\text{para}} - H_{\text{dia}}$ for constant frequency.⁶¹

(61) Horrocks, W. DeW., Jr. In *NMR of Paramagnetic Molecules: Principles and Applications*, LaMar, G. N., Horrocks, W. DeW., Jr., Eds., Academic: New York, 1973; p 137.

(62) This equation is often written in a form containing a $3kT$ term^{55,56,59} instead of a $6S_kT$ term^{57,58} in the denominator. Inclusion of the factor $2S$ leads to its definition either as $2S^m$, the total number of spins, or as the number of spins, $2S^a$, involved in the particular delocalization mechanism which gives rise to the observed contact shift.⁶³

(63) La Mar, G. N. *Inorg. Chem.* **1971**, *10*, 2633–2635.

measurements of the isotropic shifts and evaluations of g and A_i . Alternatively, a separate evaluation of ΔG at a given temperature was acquired⁵³⁻⁵⁷ from magnetic moment measurements (via the Evans method³²) on the equilibrium solution through the relationship $N_t = \mu_{\text{obsd}}^2/\mu_i^2 = [\exp(\Delta G/RT) + 1]^{-1}$, where μ_{obsd} and μ_i are the magnetic moment of the equilibrium mixture and the magnetic moment of the triplet-state tetrahedral isomer, respectively.

A subsequent analysis by McGarvey⁶⁴ of the theory for the contact shift and dipolar shift in the ^1H NMR spectra of the planar-tetrahedral equilibrium in Ni(II) complexes called into question the validity of the latter two assumptions (given above) in calculating ΔH and ΔS values via the contact-shift equation; McGarvey⁶⁴ showed that both the contact and dipolar shifts may depart markedly from T^{-1} behavior previously assumed for tetrahedral Ni(II) complexes and that the dipolar shift may in some cases be quite large. His conclusions were later critiqued by Holm and Hawkins,⁵⁷ who maintained that the isotropic shifts of most or all of the protons in these molecules derive principally from contact interactions.

Independent measurements of A_i and ΔG can be achieved only if it is possible to reach both the non-Curie ($N_t < 1$) and Curie ($N_t = 1$) regions of contact-shift dependence within the experimentally accessible temperature range of measurement.⁵⁵⁻⁵⁷ In the case of the singlet-triplet equilibrium measurements of **1** in solution, only the former limiting condition ($N_t < 1$) is clearly applicable such that no independent measurement of A_i was possible. Hence, the contact-shift equation used to fit the temperature-dependent frequency-shift data of the i th proton nucleus was rewritten as $\Delta\gamma_i = (K'\gamma_0/T)N_t = (K'\gamma_0/T)[\exp(\Delta G/RT) + 1]^{-1}$, where $K' = -A_i(\gamma_e/\gamma_H)(g\beta S(S+1)/6Sk)$ is a constant for a given proton nucleus. A least-squares fit of 26 measured $\Delta\gamma_i$'s at different T 's to the above equation (which yielded a constant $K'\gamma_0$ and a ΔG value for the methyl proton data) gave an extremely poor fit of the data, thereby implying that ΔG is not independent of temperature. A least-squares fit of the 26 $\Delta\gamma_i$'s at different temperatures to the modified equation $\Delta\gamma_i = K'\gamma_0/T[\exp\{(\Delta H - T\Delta S)/RT\} + 1]^{-1}$ produced the curve displayed as a dark line in Figure 10. The overall agreement with the experimental data is excellent over the entire temperature range of 192 K. The converged least-squares parameters are $K'\gamma_0 = 7.1(3) \times 10^5$ Hz·K, $\Delta H = 18.1(4)$ kJ/mol, and $\Delta S = 50.2(2)$ J/(mol·K). The fact that ΔH is endothermic gives rise to the thermodynamically stable isomer of **1** in solution at low temperature being the singlet-state species. The large entropy value results in the triplet-state isomer existing in significant portions in solution at higher temperatures. On the basis of the determined values for ΔH and ΔS , the calculated mole fraction of the triplet (N_t) in solution was found to vary dramatically over the temperature range investigated, viz., from an N_t value of 0.001 at 170 K, to an N_t value of 0.01 at 200 K, to an N_t value of 0.11 at 270 K, to an N_t value of 0.31 at 320 K, and to an N_t value of 0.55 at the highest measured temperature of 370 K.

Our use of the rewritten contact-shift equation, which is based on the assumption that the temperature-dependent isotropic shifts of **1** are principally contact in origin, appears to be justified. In the cases of both the 46-electron **1** and the 50-electron $\text{Co}_3(\eta^5\text{-C}_5\text{H}_5)_3(\mu_3\text{-S})_2$ ⁵⁰ and its $\text{Co}_3(\eta^5\text{-C}_5\text{H}_4\text{Me})_3(\mu_3\text{-S})_2$ analogue,⁵² the triplet-state isomer in solution is presumed to have a D_{3h} Co_3X_2 core geometry ($\text{X} = \text{CO}, \text{S}$); indeed, this axially symmetric Co_3S_2 architecture was shown^{50,51} to exist in the solid-state room-temperature phase of $\text{Co}_3(\eta^5\text{-C}_5\text{H}_5)_3(\mu_3\text{-S})_2$ which possesses two unpaired electrons. A triplet-state isomer of D_{3h} symmetry requires an orbitally nondegenerate $^3A_2'$ ground state, for which dipolar shifts are usually considered to be negligible.^{57,65} The dominance of the contact interactions in the above three trimetal bicapped clusters is also consistent with the hydrogen protons attached to

the ring carbon atoms undergoing upfield shifts with increasing temperature, whereas the methyl protons shift in the opposite direction (downfield). This reversal in isotropic shift when a hydrogen atom is replaced by a methyl group is in harmony with a spin-polarization mechanism.^{57,65}

The diamagnetic-corrected value of $\mu_{\text{eff}} = 1.45 \mu_B$ (i.e., $1.1 \mu_B$ before correction for both cobalt and ligand core effects³³) obtained by the Evans method³² for the room temperature (23 °C) magnetic moment of **1** in solution is in reasonable agreement with the value of $1.3 \mu_B$ calculated from the equation $N_t = (\mu_{\text{eff}}^2/\mu_i^2) = [\exp(\Delta H - T\Delta S)/RT + 1]^{-1}$, where the magnetic moment μ_i for the triplet-state isomer was assumed to have a spin-only value of $2.83 \mu_B$. The corresponding N_t values for the triplet-state isomer in solution at 23 °C are 0.26 from the Evans method vs. 0.21 from the ^1H NMR isotropic-shift method.

Structural-Bonding Interrelationships of $\text{Co}_3(\eta^5\text{-C}_5\text{Me}_5)_3(\mu_3\text{-CO})_2$ (1**), $\text{Rh}_3(\eta^5\text{-C}_5\text{Me}_5)_3(\mu_3\text{-CO})_2$ (**2**), and the Isolobal Cyclopropenyl Monoanion.** (a) **General Comments.** A correlation between structure and electronic configuration is especially intriguing for **1** and **2** in that (1) previous theoretical predictions were made by Hoffmann and colleagues^{23,24} that the hypothetical 46-electron $\text{M}_3(\eta^5\text{-C}_5\text{H}_5)_3(\mu_3\text{-CO})_2$ clusters ($\text{M} = \text{Co},^{23} \text{Rh}^{24}$) should possess two unpaired electrons in the half-filled e' HOMOs (Figure 1) under D_{3h} symmetry and (2) **1** and **2** are isolobal with the highly unstable (and non-isolobal) cyclopropenyl monoanion⁶⁶ which is the simplest known 4π electron, antiaromatic triplet-state species under D_{3h} symmetry.¹⁷

Although all three of these triangular ring systems possess the same triplet ground state (viz., $^3A_2'$) under assumed D_{3h} symmetry with two unpaired electrons, each appears to undergo a different geometrical distortion in order to split the doubly degenerate, half-filled HOMOs and thereby attain a singlet ground state.

(b) **The $[\text{C}_3\text{H}_3]^-$ Monoanion.** Nonempirical calculations⁶⁷ suggested a singlet ground state that is associated with a nonplanar C_s - m geometry with two carbon atoms forming an ethylenic π bond and with a lone pair of electrons localized on the third highly pyramidalized carbon atom.

(c) **$\text{Rh}_3(\eta^5\text{-C}_5\text{Me}_5)_3(\mu_3\text{-CO})_2$ (**2**).** Its crystal-ordered configuration (Figure 8), determined from the low-temperature X-ray diffraction analysis by Howard,^{20a,b} shows a marked distortion of the $\text{Rh}_3(\text{CO})_2$ core from a D_{3h} toward a C_{2v} geometry with one long and two short Rh-Rh bond lengths and with four short and two long Rh-CO bonding distances. The differences between the means for the two sets of bond lengths (averaged under C_{2v}

(66) The use of the isolobal concept^{5,12} to describe the cycloaddition reactions² of the ethylene-like $\text{Co}_2(\eta^5\text{-C}_5\text{Me}_5)_2(\mu_2\text{-CO})_2$ dimer with methylene-like 16-electron metal fragments to yield trimetal systems analogous to cyclopropane prompted us to determine the simple organic analogue of **1**. The cycloaddition of the 14-electron $\text{Co}(\text{C}_5\text{Me}_5)$ fragment to $\text{Co}_2(\eta^5\text{-C}_5\text{Me}_5)_2(\mu_2\text{-CO})_2$ to give $\text{Co}_3(\eta^5\text{-C}_5\text{Me}_5)_3(\mu_3\text{-CO})_2$ (**1**) corresponds to the cycloaddition of $[\text{CH}]^+$ to C_2H_4 to give the hypothetical $[\text{C}_3\text{H}_3]^+$ monocation which is isolobal to the $[\text{C}_3\text{H}_3]^-$ monoanion by removal of two protons. A more illustrative construct results from the assemblage of three $\text{Co}(\text{C}_5\text{Me}_5)$ -like $[\text{CH}]^+$ moieties to give the $[\text{C}_3\text{H}_3]^{3+}$ trication which is electronically equivalent to the $\text{Co}_3(\text{C}_5\text{Me}_5)_3$ fragment; the formation of the $[\text{C}_3\text{H}_3]^-$ monoanion by the addition of four electrons to the π -system of the $[\text{C}_3\text{H}_3]^{3+}$ trication corresponds to the isolobal formation of **1** by the addition of two capping CO ligands as two-electron σ -donors to the $\text{Co}_3(\text{C}_5\text{Me}_5)_3$ fragment.

(67) Potential surfaces for the lowest triplet and two lowest singlet states of the (unknown) triaziridenyl dication, $[\text{N}_3\text{H}_3]^{2+}$, which is isoelectronic with the $[\text{C}_3\text{H}_3]^-$ monoanion, were recently obtained from sophisticated ab initio σ - π CI calculations.^{17e} The selection of the unknown isoelectronic $[\text{N}_3\text{H}_3]^{2+}$ dication for a comprehensive theoretical analysis^{17e} was made on the basis that (unlike the case of the $[\text{C}_3\text{H}_3]^-$ monoanion) all of its electrons would be bound in the gas phase. The calculations led to the prediction that the $[\text{N}_3\text{H}_3]^{2+}$ dication should have a singlet ground state with a nonplanar C_s - m geometry consisting of two nitrogen atoms forming an ethylenic-like π bond and a third highly pyramidalized nitrogen atom possessing a lone pair of electrons. These calculations also indicated a high activation barrier for pseudorotation of the $[\text{N}_3\text{H}_3]^{2+}$ dication between the three equivalent minima on the singlet energy surface. Borden and Davidson^{17e,f} suggested that the isoelectronic cyclopropenyl monoanion in solution may likely possess a singlet ground state resulting from a similar nonplanar C_s geometry. In fact, from earlier nonempirical SCF calculations based upon the known C-C bond lengths of cyclopropene, Clark^{17b} had proposed the same nonplanar C_s architecture for the $[\text{C}_3\text{H}_3]^-$ monoanion with a localized electron pair on the unique pyramidal carbon atom whose C-H bond was bent at 68° to the plane of the carbon ring.

(64) McGarvey, B. R. *J. Am. Chem. Soc.* **1972**, *94*, 1103-1108.

(65) Horrocks, W. DeW., Jr. In *NMR of Paramagnetic Molecules: Principles and Applications*; La Mar, G. N., Horrocks, W. DeW., Jr., Holm, R. H., Eds.; Academic: New York, 1973; pp 127-177.

symmetry) are 0.08 Å for the Rh–Rh bond lengths and 0.36 Å for the Rh–CO bond lengths. This particular C_{2v} deformation from D_{3h} geometry corresponds to one of the distortions proposed by Hoffmann and colleagues²⁴ in 1980 in order for the hypothetical $Rh_3(\eta^5-C_5H_5)_3(\mu_3-CO)_2$ to possess a singlet ground state. The fact that Stone and co-workers¹⁹ observed that ¹³C NMR spectra of the compound at –70 °C exhibited a symmetric quartet for the triply bridging carbonyl carbon resonance led to their proposal of fluxional behavior for **2** in solution. Since **2** differs from **1** in *not* exhibiting a paramagnetic-induced shift of its single methyl proton resonance in solution, rapid interconversion of the three C_5Me_5 ligands under C_{2v} symmetry can occur on the NMR time scale via a low-energy pathway involving only singlet-state species.

The abnormal thermal ellipsoids shown in Figure 7 for the crystal-disordered geometry of **2** obtained by us from the room-temperature crystallographic study clearly signify that it is the mirror-disordered composite of the actual low-temperature C_{2v} geometry. The unusually high discrepancy factors obtained for this refined structure provide additional crystallographic evidence for the presence of large systematic errors in the structural determination.

(d) $Co_3(\eta^5-C_5Me_5)_3(\mu_3-CO)_2$ (**1**). The well-refined crystal structure of **1**, in which the cluster is constrained to $C_{3h}-3/m$ site symmetry, provides no indication that its atomic thermal ellipsoids (Figures 4 and 5) are a threefold composite of a markedly distorted $Co_3(CO)_2$ core. However, the C_5Me_5 ligands in **1** appear to be significantly deformed from a regular pentagonal geometry, as evidenced by a maximum variation of 0.095 Å among the three independent C–C bond lengths in the mirror-bisected C_5Me_5 ring. Hence, we propose that the absence of a large solid-state magnetic moment characteristic of two unpaired electrons for **1** at room temperature may be a consequence of the breakdown in orbital degeneracy resulting mainly from unsymmetrical interactions of the C_5Me_5 ligands with the $Co_3(CO)_2$ core such that the “instantaneous” molecular configuration does *not* possess threefold symmetry. This indication that the C_5Me_5 ligands play a dominant role in accounting for the singlet ground state of **1** is not surprising in light of similar dependencies of spin-state configurations on cyclopentadienyl ring deformations having been found^{68,69} for metallocenes (in which the deformed C_5Me_5 rings drastically lower the molecular symmetry to a point group containing no principal axis of higher than twofold symmetry). This indicated difference (and/or degree) in geometrical distortion between **1** and **2** may

reflect the much weaker metal–metal vs. metal–ligand bonding interactions for the cobalt atoms compared to the rhodium atoms.

An operational test of our hypothesis would involve the synthesis and structural-bonding analysis of a 46-electron analogue of **1**, $Co_3(\eta^5-C_5Me_4R)_3(\mu_3-CO)_2$ (where R = Et or *i*-Pr). The C_5Me_4R rings should give rise to the analogue possessing general crystallographic C_1-1 site symmetry; thus, its crystalline geometry should reflect the “instantaneous” (instead of “threefold-averaged”) configuration. Temperature-variable solid-state magnetic susceptibility and proton NMR measurements would also be necessary to establish the extent of its paramagnetism and whether it exhibits a temperature-dependent singlet–triplet solution equilibrium.

Acknowledgment. This research was generously supported by a grant from the National Science Foundation. We are greatly indebted to Dr. Judith Howard (Department of Inorganic Chemistry, the University of Bristol) for supplying us with the results of her low-temperature X-ray determination of the crystal structure of $Rh_3(\eta^5-C_5Me_5)_3(\mu_3-CO)_2$, including a drawing of its molecular configuration and selected bond lengths. We gratefully acknowledge Professor F. Gordon A. Stone (Department of Inorganic Chemistry, the University of Bristol) for providing us with a preprint of his comprehensive article (in *Angew. Chem.*) on Metal–Carbon and Metal–Metal Multiple Bonds as Ligands in Transition-Metal Chemistry: The Isolobal Connection and for his interest in our research. Special thanks are due to Dr. R. B. Cody (Nicolet Analytical Instruments) for obtaining definitive mass spectral data on $Co_3(\eta^5-C_5Me_5)_3(\mu_3-CO)(\mu_3-O)$ with a Nicolet FT MS-1000 mass spectrometer. We also appreciate helpful discussions with Dr. Robert L. Bedard on electrochemical measurements and with Dr. Kimberly A. Schugart on bonding aspects of the $Co_3(\eta^5-C_5Me_5)_3(\mu_3-CO)_2$ cluster gleaned from nonparametrized MO calculations with the Fenske–Hall model.

Registry No. **1**, 96892-45-4; **2**, 88297-70-5; **3**, 104779-45-5; $Fe_2(\eta^5-C_5H_5)_2(CO)_2(\mu_2-CO)_2$, 12154-95-9; $Co(\eta^5-C_5Me_5)(CO)_2$, 12129-77-0; $Co_2(\eta^5-C_5Me_5)_2(\mu_2-CO)_2$, 69657-52-9; $Fe_2Co(\eta^5-C_5H_5)_2(\eta^5-C_5Me_5)(CO)_4$, 84462-59-9; $Co(\eta^5-C_5Me_5)(C_2H_4)_2$, 80848-36-8; $Co_2(\eta^5-C_5Me_5)(\mu_2-CO)_2$, 69657-52-9; $Fe(\eta^5-C_5H_5)(CO)_2Me$, 12080-06-7; $[Co(\eta^5-C_5Me_5)I_2]_2$, 72339-52-7; $Rh_2(\eta^5-C_5Me_5)_2(\mu_2-CO)_2$, 69728-34-3; ethylene, 74-85-1; Co, 7440-48-4; Ru, 7440-18-8.

Supplementary Material Available: Tables presenting calculated coordinates and isotropic temperature factors for all hydrogen atoms and anisotropic thermal parameters for all non-hydrogen atoms (1 page); a table listing observed and calculated structure factor amplitudes (4 pages). Ordering information is given on any current masthead page.

(68) Freyberg, D. P.; Robbins, J. L.; Raymond, K. N.; Smart, J. C. *J. Am. Chem. Soc.* **1979**, *101*, 892–897.

(69) Ammeter, J. H., *J. Mag. Reson.* **1978**, *30*, 299–325.